The Occlusion Process in a Midlatitude Cyclone over Land

DAVID M. SCHULTZ* AND CLIFFORD F. MASS

Department of Atmospheric Sciences, University of Washington, Seattle, Washington

(Manuscript received 5 December 1991, in final form 13 July 1992)

ABSTRACT

A historical review highlights the lack of consensus regarding the structure and evolution of occluded fronts and cyclones. In order to better understand the occlusion process, this paper and its companion examine a model simulation of the 14–16 December 1987 cyclone over the eastern United States. The structure of an occluded front was observed at low levels as the cold front caught up with the warm front, while aloft an upper-level frontal zone appeared to play a role in the occlusion process. Although the thermal structure of this storm suggested that a cold-type occlusion should have formed, the model simulation produced a warm-type occlusion structure. An extensive review of the literature on occluded fronts suggested that cold-type occlusions are rare, if they exist at all. Finally, the occluded front simulated in this case is compared critically to the Norwegian, "T-bone," and other conceptual models of cyclone evolution.

1. Introduction

Since proposed by Bjerknes and Solberg in 1922, the classical model of cyclone evolution and occlusion, in which a cold front overtakes a warm front, has been challenged in many ways. Some scientists have found structures on the meso-α and meso-β scales that were not predicted by the Norwegian cyclone model (e.g., Kreitzberg 1964, 1968; Hobbs et al. 1975; Houze et al. 1976). Others have suggested that the essential feature of an occlusion is the trough of warm air aloft, not the surface position of the occluded front (e.g., Godson 1951; Penner 1955; Galloway 1958). Still others have shown that occluded frontal structure can occur without the classical occlusion process (e.g., Douglas 1929; Palmén 1951; Arakawa 1952; Reed 1979; Locatelli et al. 1989). Finally, some investigators have suggested that little evidence exists to support the ideal occlusion model in which a cold front overtakes a warm front (e.g., Wallace and Hobbs 1977; Shapiro and Keyser 1990).

Even today, the nature of the occlusion process is still not well understood. As noted by Keyser (1986), one factor in the apparent lack of progress is that "modern case studies illustrating occluded fronts and the occlusion process are virtually nonexistent." In addition, the lack of spatial and temporal resolution of the observing network has made the detailed study of the occlusion process difficult.

This study attempts to address several of the issues noted above by examining a high-resolution model simulation of the occluding cyclone of 14–16 December 1987. Mass and Schultz (1993) examine both the observed and simulated large-scale evolutions of this storm from a synoptic perspective, while this paper describes the occlusion process in detail. Although reading Mass and Schultz (1993) is useful for obtaining familiarity with the particulars of this case, this paper may be read independently of its counterpart.

The remainder of the paper is organized in the following manner. Section 2 outlines the historical development of thought regarding occluded fronts and cyclones. In section 3, the mesoscale model that simulated this storm is briefly described. Section 4 consists of a multifaceted examination of the simulated occluded front including vertical cross sections and trajectory analysis. In section 5, this cyclone is discussed in relation to different conceptual models of cyclone evolution. Finally, a summary is provided in the last section.

2. Review of previous studies on occluded fronts

a. The ideal cyclone model

The occlusion process was first identified by Bergeron while studying the cyclone of 18 November 1919[1] and was incorporated into the conceptual model of midlatitude cyclone evolution presented by Bjerknes

* Current affiliation: Department of Atmospheric Science, ES-219, State University of New York at Albany, Albany, NY 12222.

Corresponding author address: Clifford F. Mass, Department of Atmospheric Sciences, AK-40, University of Washington, Seattle, WA 98195.

[1] His analyzed surface map for this case can be found in Bergeron (1959). The original drawing can be found in Jewell (1981).

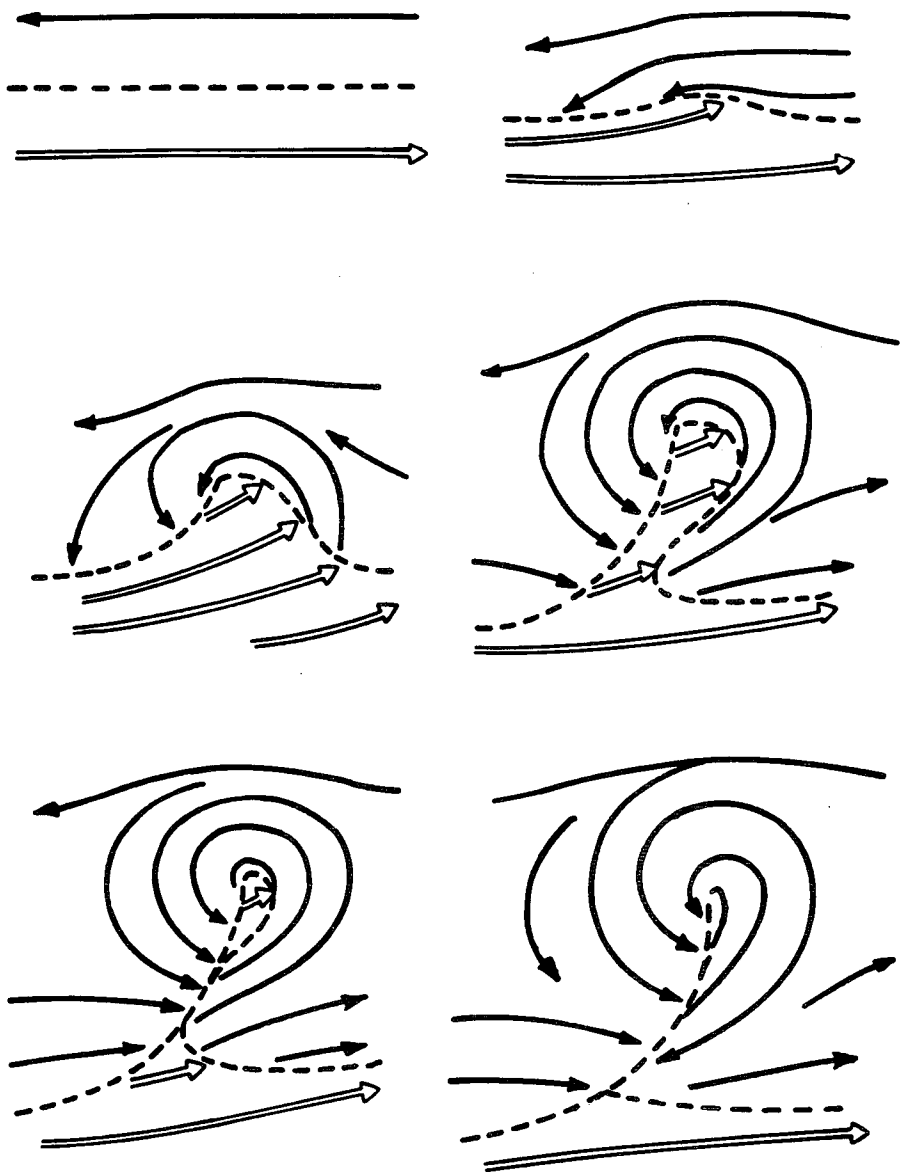

FIG. 1. The life cycle of an extratropical cyclone (after Bjerknes and Solberg 1922). Solid lines indicate streamlines and dashed lines signify frontal boundaries.

and Solberg (1922). In their model (Fig. 1), a wave on the preexisting polar front amplifies. The resulting cold front rotates around the developing low center and overtakes a warm front, forcing the intervening warm sector air aloft. The surface where the two fronts meet is called the *occluded front* or *occlusion.* In areas of topography, this catch-up can potentially occur south of the peak of the warm sector, leaving an area of *secluded* warm-sector air near the cyclone center.[2] Eventually the secluded warm air is removed from the surface, leaving a wedge of warm air aloft. Bjerknes and Solberg also noted that after occlusion, the cyclone soon begins to weaken.

Bjerknes and Solberg (1922) first considered an ideal occlusion structure in which no thermal boundary

[2] In several of the cases studied by the Norwegian school, this seclusion process was caused by the retardation of the warm front by the Skagerak peninsula of Norway. The situation whereby the occlusion process is hastened by the slowing of the warm front along the windward slopes of a mountain range is termed an *orographic occlusion* (Huschke 1959). It is interesting to note that Bergeron (1928, 1937) originally defined the orographic occlusion as the retardation of an advancing cold front by a mountain range, a process having little in common with the traditional occlusion process. The development of this terminology is confusing and uncertain.

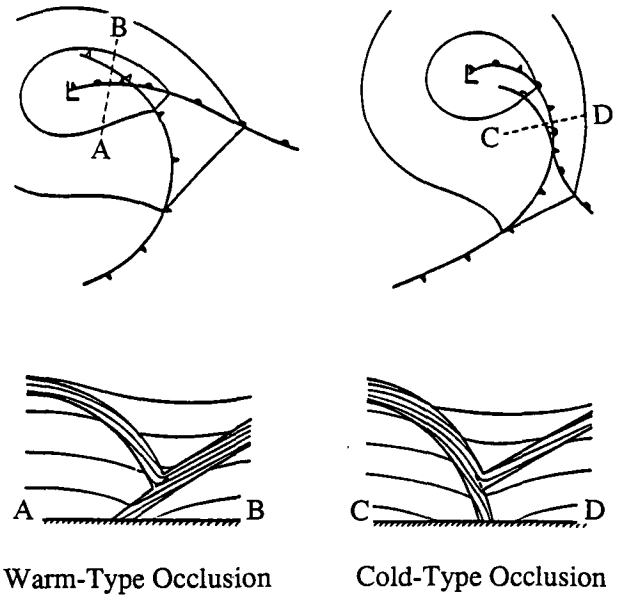

FIG. 2. Vertical cross sections and surface maps through warm-type and cold-type occlusions (Saucier 1955). Cross sections *AB* and *CD* display potential temperature and frontal boundaries.

formed at any height. They admitted that such a *neutral occlusion* (Godske et al. 1957; Huschke 1959) would not usually be observed. Sometimes the polar air in the rear of the cyclone is warmer than the polar air in front of the cyclone, producing what was later termed a *warm-front occlusion, warm-type occlusion, warm-front-type occlusion,* or *warm occlusion* (Fig. 2). Alternatively, if the air behind the cold front is colder than the air in front of the warm front, a *cold-front occlusion, cold-type occlusion, cold-front-type occlusion,* or *cold occlusion* forms. Bjerknes and Solberg suggested that cold-type occlusions should be more common than warm-type occlusions because the air to the west of the cyclone center arrives more directly from the north and thus is colder.[3]

Bjerknes and Solberg (1922) called their proposed paradigm of cyclone evolution *the ideal cyclone model.* For the sake of convenience in this paper, an "ideal," "Norwegian," or "classical" cyclone is one that develops according to the ideal model presented by the Norwegian school.

Bergeron (1937), following Bjerknes (1930), presented the concept of a *retrograde occlusion* (later called the *back-bent, loop, broken-back,* or *bent-back occlusion*), which supposedly formed as the low center traveled down the length of the occluded front toward the peak of the warm sector [Bergeron (1937) referred to the section of occluded front south of the low center as the *direct occlusion*]. Later the term *bent-back occlusion* became used for the segment of an occluded front that reverses its direction of motion between the primary cyclone and a secondary development at the peak of the warm sector (Petterssen 1940; Huschke 1959). This term has also been applied to secondary troughs (in sea level pressure) that often develop to the rear of cyclones (Petterssen 1956).

b. Objections to the ideal model of occlusion

Soon after the ideal cyclone model was proposed, Douglas (1929) raised objections, claiming that a structure resembling an occlusion can be present without a preexisting warm sector. Specifically, he observed a developing cyclone within polar air that formed an occluded-like structure. Arakawa (1952) studied Typhoon Ruth, during which an occluded-like structure formed as a result of the interaction between a warm front associated with the typhoon and an extension of the polar front to the northeast. In Palmén (1951), a cold front associated with an eastward-moving cyclone joined with a preexisting stationary front along the Gulf Coast to form an occluded wave. This case has been referred to as Palmén's *pseudo-occlusion.* In each example described above, the resulting structure resembled an occluded front, yet none appeared to form in the classical manner.

In a systematic critique of the Norwegian cyclone model, Postma (1948) pointed out that back-bent occlusions were often not genuine fronts and could be better explained by surface pressure troughs within the cold air to the rear of the cyclone center.[4] Postma also suggested that Norwegian analysts, faced with the separation of the low center from the peak of the warm sector at the surface, drew an occluded front in the gap despite any evidence that the occlusion process had ever occurred. Finally, he added that often an occlusion was analyzed when the shape of the warm sector had not changed; in his words, "an occlusion is added as an accretion."

German (1959), studying the occlusion process at the earth's surface, concluded that the warm air could not have been advected as far north as the occlusion was drawn and that the occluded front at the surface could not have formed ideally. German conceded, however, that at 850 mb, the occlusion was not inconsistent with the ideal model.

Godson, Penner, Galloway, and their colleagues at the Canadian Meteorological Service observed that often there was no significant temperature difference

[3] Bjerknes (1951) added that later in the evolution of a cyclone, the warm-type occluded structure may transform to a cold-type structure along the southern part of the occluded front.

[4] As noted above, Petterssen (1956) also recognized these back-bent occlusions or secondary cold fronts as surface troughs that were associated with short waves aloft. These cold troughs, he argued, consisted of air of rather homogeneous properties. Thus, to introduce a frontal structure would be "a misuse of the concept of fronts" (Petterssen 1956). Andersen (1978), however, believed that true back-bent occlusions with warmer air aloft actually existed.

across an occluded front in the lower troposphere and that the largest temperature contrast, as well as the most significant weather, were located above the surface.[5] They suggested that the projection to the surface of the base of the warm-air trough aloft, termed the *trowal*—trough of warm air aloft—is more meaningful than small wind or temperature changes at the earth's surface. Galloway (1958) identified the passage of a trowal with rapid clearing of middle and high clouds, a change from prefrontal precipitation to airmass showers, and a trough in sea level pressure. In fact, Godson (1951) boldly stated that "this [trowal] model completely and adequately fits at least 95 per cent of all occluded frontal waves crossing the West Coast of North America." Galloway (1960) also observed that the motion of the cyclone center decreased or even stopped during occlusion and that deepening may continue even after the occluded front at the surface appeared. Indeed, deepening of a cyclone after it is said to have occluded can be observed frequently on contemporary weather maps. This contrasts with Bjerknes and Solberg (1922), who suggested that after occlusion a cyclone soon begins to fill up.

In their introductory textbook, Wallace and Hobbs (1977) stated that "when actual frontal movements are carefully examined, there are few, if any, well-documented examples of cold fronts overtaking warm fronts to form occlusions." Instead of the classical "catch-up" mechanism of occluded-front formation, they suggested that the surface low separates itself from the junction of the warm and cold fronts and continues to deepen back into the cold air, with an occluded front connecting the low center to the peak of the warm sector. Thus, an occluded front is essentially a new front. Wallace and Hobbs, however, did not outline the mechanism(s) by which such an occlusion process occurs.

Several studies have shown that parts of the classical occluded frontal structure may be absent. For example, Elliott (1958), studying cold-type occlusions over the California coast, found no clear indication of an elevated warm-frontal surface within 150 miles of the surface front. Kuo and Reed (1988) claimed that their storm did not occlude in a classical manner because of the weakness of the warm front. Wallace and Hobbs (1977) recognized that frontal surfaces may either be absent or obscured by mesoscale activity. As noted in the next section, several field programs have found occlusion structures substantially different from the ideal.

c. *Mesoscale field experiments*

Kreitzberg (1964), using serial ascents and vertically pointing radar, examined the subsynoptic structures of five occlusions passing over the Pacific Northwest. For older warm-type occlusions, he found that after the passage of the elevated cold front, the stable warm-frontal zone dissipated and never reached the surface. The only significant weather features were related to a mesoscale secondary cold front behind the primary cold front aloft. In contrast, the younger occlusions were nearly vertical through the lower troposphere and were often split. These splits, Kreitzberg argued, can be associated with squall lines, secondary cold fronts, and pre- and postfrontal rain bands.

Further studies by Kreitzberg (1968) and Kreitzberg and Brown (1970), based on observations from Project Stormy Spring in New England, described the mesoscale structure of a pseudo-occlusion (Palmén 1951). Kreitzberg (1968) identified several mesoscale features associated with this occlusion, including a 120–250-mb-thick stable layer corresponding to the warm frontal zone, two warm tongues associated with the upper boundary of the stable layer, a prefrontal surge of cold dry air aloft, the occluded front that signified the end of warm advection and the onset of cold advection, the primary cold front, and three secondary cold fronts following the primary front (Fig. 3).

The CYCLES (Cyclonic Extratropical Storms) Project at the University of Washington in the 1970s yielded new insights into the mesoscale structures of occluded cyclones. For example, Hobbs et al. (1975) observed an occlusion that had no broad stratiform precipitation ahead of the occluded front, as was usually present, and noted the prefrontal surge of Kreitzberg (1968). The "prefrontal waves" of Elliott and Hovind (1965), the "warm tongues" of Kreitzberg (1968), or equivalently, the "mesoscale frontal interfaces" of Matkovski and Shakina (1982) were also identified. These warm tongues were separated by approximately 220 km, which agreed quite well with the previous case studies. Saarikivi and Puhakka (1990) confirmed the existence of similar mesoscale features in a serial ascent study over Southern Finland. Hobbs et al. (1975) also observed weak baroclinic zones in the cold air behind the system. These structures resembled the secondary cold fronts observed by Kreitzberg (1968).

Occluded fronts during CYCLES were also analyzed by Houze et al. (1976) and Hertzman and Hobbs (1988). In three cases during 19–21 December 1973, Houze et al. (1976) observed no clear frontal structure below 850 mb. The fragmented nature of the frontal zones was also noted, consistent with Kreitzberg's (1964) conclusions that older occluded systems lack low-level structure. Hertzman and Hobbs (1988) used dual-Doppler analyses to document the three-dimensional airflow within a young warm-type occlusion.

Yet another mesoscale–synoptic experiment was GALE (Genesis of Atlantic Lows Experiment). Although primarily focusing on explosive cyclogenesis, several weak occlusion-like features were observed and subsequently analyzed. For example, Locatelli et al.

[5] Penner (1955) noted that "an occluded front which can actually be verified by aerological data is one of the rarer meteorological phenomena."

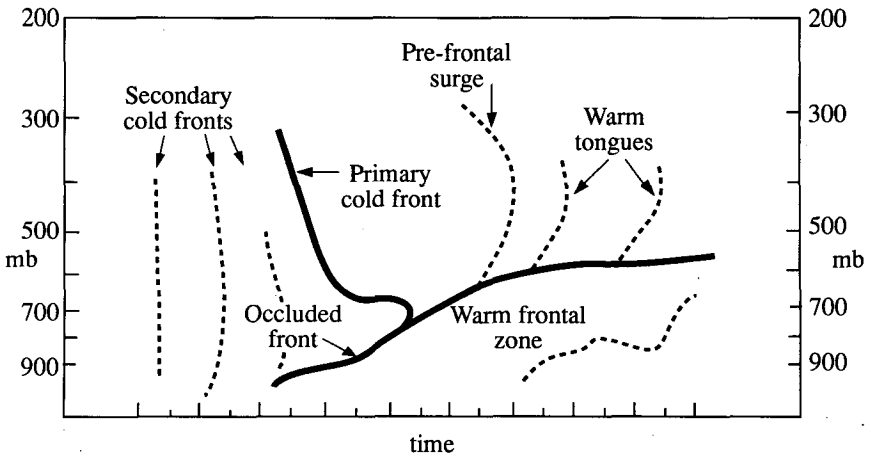

FIG. 3. Time cross section from serial ascents through an occlusion showing its mesoscale features (after Kreitzberg 1968).

(1989) described the structures that formed as a cold front overtook an evolving lee trough (Fig. 4). This structure was similar to a warm-type occlusion in two ways. First, there were multiple pushes of cold air aloft as found in other examples (e.g., Elliott and Hovind 1965; Kreitzberg 1968). Second, the equivalent potential temperature, temperature, wind, and humidity fields were similar to those found in warm-type occlusions. Because there was technically no warm front, Locatelli et al. (1989) refrained from using occluded

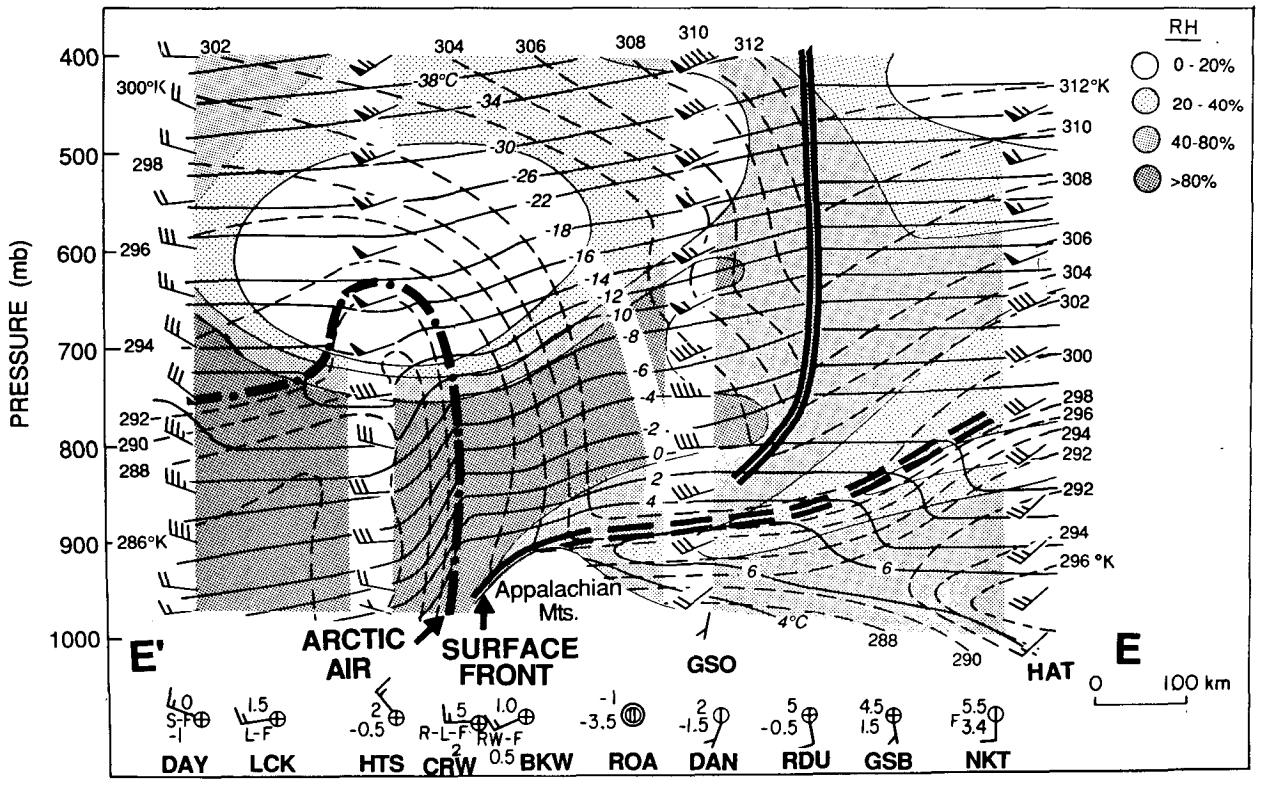

FIG. 4. Cross section of a warm-type occluded structure formed as a cold front went aloft over a lee trough (Locatelli et al. 1989). Air temperature (solid) and θ_e (dashed) shown with 4°C and 2-K contour intervals, respectively. Relative humidity (%) indicated by shading (see inset). The leading edge of cold advection is marked by two bold lines, the leading edge of Arctic air is marked by a dot–dash line, and a double-dash line signifies the cold side of the zone of warm advection.

frontal symbols or referring to it as a warm-type occlusion. "Clearly," they said, "new definitions and classifications of fronts and frontal systems, or careful clarification of present definitions, are needed."

d. The "instant" occlusion

On many occasions, satellite imagery has suggested that occlusions or occluded-like structures might form in nonclassical ways. Anderson et al. (1969) identified the *instant occlusion* that occurs if a comma cloud, associated with positive vorticity advection aloft, approaches and merges with a frontal wave. The structure that forms appears to be an occluded front but without a history of frontal "catch-up." As Reed (1979) pointed out, the frontal wave provides the warm and cold fronts, while the comma cloud contributes the low pressure center and occluded front. Subsequent work by Locatelli et al. (1982) suggested that the comma cloud provides not only the low pressure center and the occluded front, but a cold front as well. Carleton (1985) showed that at both 500 and 300 mb, two distinct geopotential anomalies exist—one representing the comma cloud and the other associated with the incipient frontal wave. A case study by Mullen (1983) of an instant occlusion showed the interaction of two surface low centers and the formation of an occluded front between them. Although Mullen (1983) recognized that the introduction of this front was rather arbitrary, he argued that frontogenesis had occurred as a result of the intensification of the horizontal wind shear in the region between the two low centers.

Browning and Hill (1985) analyzed a case resembling an instant occlusion and presented the flow through the system using a conveyor belt model. Their case differed from the canonical instant occlusion model in that the polar front cloud mass developed simultaneously with the comma cloud rather than being a preexisting feature in the flow. Based on this one case study, Browning and Hill chose to call this system a *pseudo-occlusion* [not to be confused with Palmén's (1951) pseudo-occlusion]. Monk (1987) showed satellite imagery that appears to support Browning and Hill's conclusions.

McGinnigle et al. (1988), studying the instant-occlusion process over the North Atlantic, explained the process differently (Fig. 5). Their interpretation was that as a comma cloud approached a preexisting front, the warm advection in advance of the comma caused frontolysis of the front and frontogenesis along a second cloud band. This second cloud band then became the primary cold front of the cyclone, while the cloud mass of the original front dissipated. This evolution is consistent with Locatelli et al. (1982), who observed the polar front and the comma cloud to remain separate. Zwatz-Meise and Hailzl (1983) independently found similar results in what they termed "the penetration of a second cloud band at the rear of a cold front."

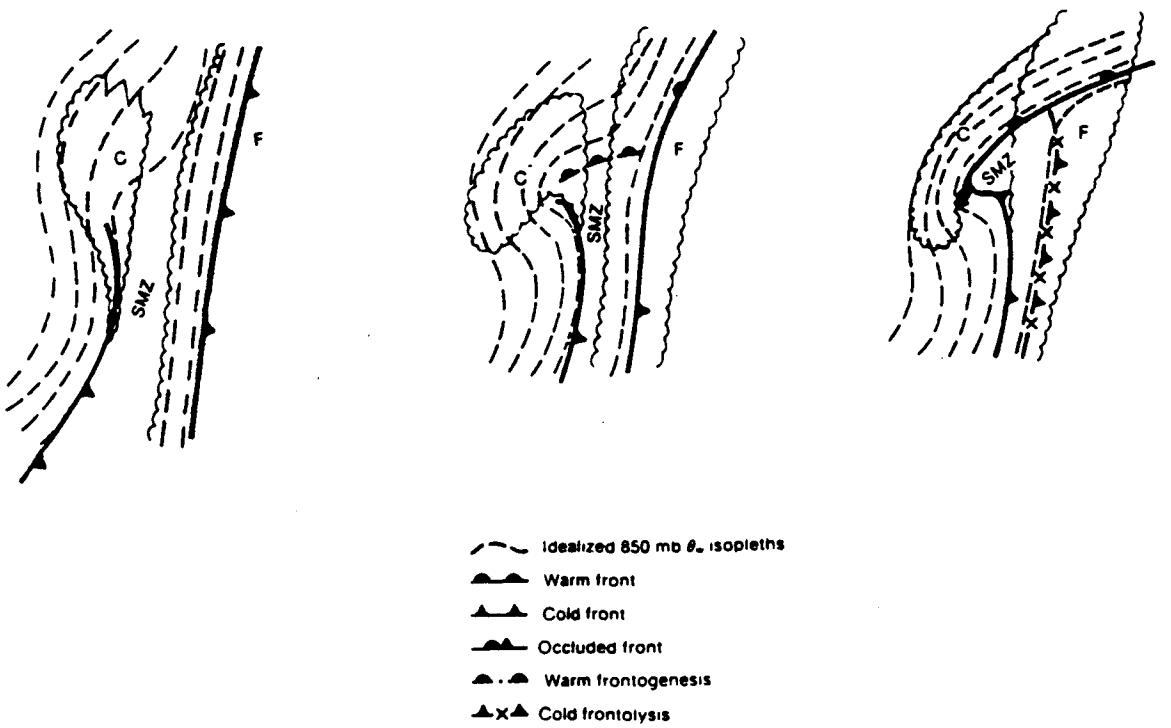

FIG. 5. Life cycle of an instant occlusion at three times (McGinnigle et al. 1988); *C* represents the polar-air cloud feature and *F* the polar frontal cloud. SMZ denotes the shallow moist zone. Stippling denotes upper cloud.

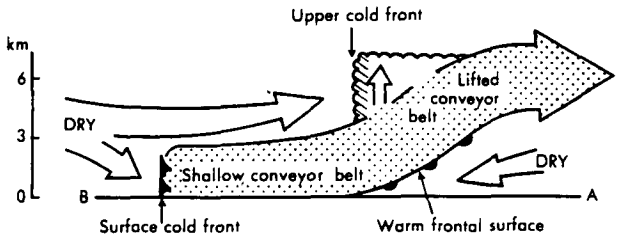

FIG. 6. Schematic of the vertical structure of a split cold front (Browning and Monk 1982).

e. *Other occluded-like structures: The split cold front and the cold front aloft*

Several other models have been proposed to account for nonclassical frontal structures that resemble occluded fronts. In a study of nine cold fronts associated with mature cyclones crossing the British Isles, Browning and Monk (1982) found an "upper cold front" up to several hundred kilometers ahead of the surface cold front. They admitted that this upper cold front was associated with a larger humidity than temperature drop and suggested that a slanting moist conveyor belt extended ahead of the surface and upper cold fronts and above a surface-based warm front. An inflow aloft of dry air from the rear of the system was found above the moist conveyor belt (Fig. 6). Browning and Monk showed that these *split cold fronts* are commonly identified as occlusions and recognized the similarity between their model and a trowal. They cited the presence of unoccluded warm air between the upper and lower fronts as the factor that distinguishes a split cold front from a trowal. McGinnigle et al. (1988) showed that cross sections across their instant occlusions resembled a split cold front.

Hobbs et al. (1990) proposed the *cold front aloft* model to explain frontal structures east of the Rocky Mountains. This feature appears to form as short waves pass over and to the lee of the Rocky Mountains. Convection often occurs as descended dry air overrides high-θ_e air east of the surface trough. Hobbs et al. (1990) suggested that this model resembles a warm-type occlusion if the surface trough is an occluded front.

f. *Shapiro and Keyser's (1990) cyclone model*

Using aircraft observations and dropwindsonde data from three field experiments that investigated marine cyclone development (the Alaskan Storm Program, pre-ERICA, and ERICA—Experiment on Rapidly Intensifying Cyclones over the Atlantic), Shapiro and Keyser (1990) documented several examples of a cyclone structural evolution that substantially differ from the ideal cyclone model (Fig. 7). In this model, as the cyclone develops, the cold front separates itself from the warm front ("*fractures*") and advances into the warm sector, while the warm front gets wrapped around in the cold northerly flow to the rear of the cyclone, forming what Shapiro and Keyser call the *bent-back warm front.* It has been suggested that the bent-back warm front is no different than the previously described bent-back occlusion (e.g., Sanders 1990, personal communication; Pike 1991). Cross sections confirm that the back-bent front has the structure of a warm front and not an ideal occluded front. Later in the cyclone's development, cold air circling around the cyclone center partially or totally encloses a region of relatively warmer air forming a *warm-core seclusion.* Note that the seclusion described by Shapiro and Keyser (1990) is different than Bjerknes and Solberg's (1922) seclusion process, which resulted from the topographic retardation of the warm front.

Several numerical simulations of cyclogenesis initialized with idealized basic states have exhibited evolutions and structures that resemble the Shapiro and Keyser model (e.g., Mudrick 1974; Hoskins 1976; Hoskins and West 1979; Takayabu 1986; Nakamura 1989; Schär 1989; Keyser et al. 1989; Polavarapu and Peltier 1990). For example, Polavarapu and Peltier (1990) used a high-resolution, dry, β-plane, nonhydrostatic, primitive equation model to simulate the nonlinear occlusion process in a frictionless environment. As the baroclinic wave amplified, the warm sector narrowed as the cold front approached the warm front (Fig. 8). By day 6, features resembling a bent-back warm front and warm-core seclusion were apparent. In a series of semigeostrophic simulations of the development of cyclonic disturbances on a broad upper westerly jet, Hoskins and West (1979) found that "none of the baroclinic waves produced an occlusion if by this is meant a cold front catching up to a warm front."

Some realistic primitive equation simulations initialized with observed data have possessed the frontal fracture and warm-seclusion structures. One example is the explosively deepening *QE II* storm of September 1978, presented in Shapiro and Keyser (1990) and Kuo et al. (1991). Not all simulations of marine cyclogenesis, however, have yielded such nonideal structures (Kuo et al. 1992). Furthermore, primitive equation simulations using surface friction appropriate to land produced structures reminiscent of the classical model (Hines and Mechoso 1992, personal communication).

g. *Summary*

The above review suggests some outstanding questions concerning occluded fronts.

- What is the basic nature of the occlusion process? Do cyclones ever occlude in the classical manner in which a cold front catches up to a warm front?
- Can the ideal occluded frontal structure be formed by nonideal mechanisms?
- Are cold fronts aloft and split cold fronts related to occluded fronts?

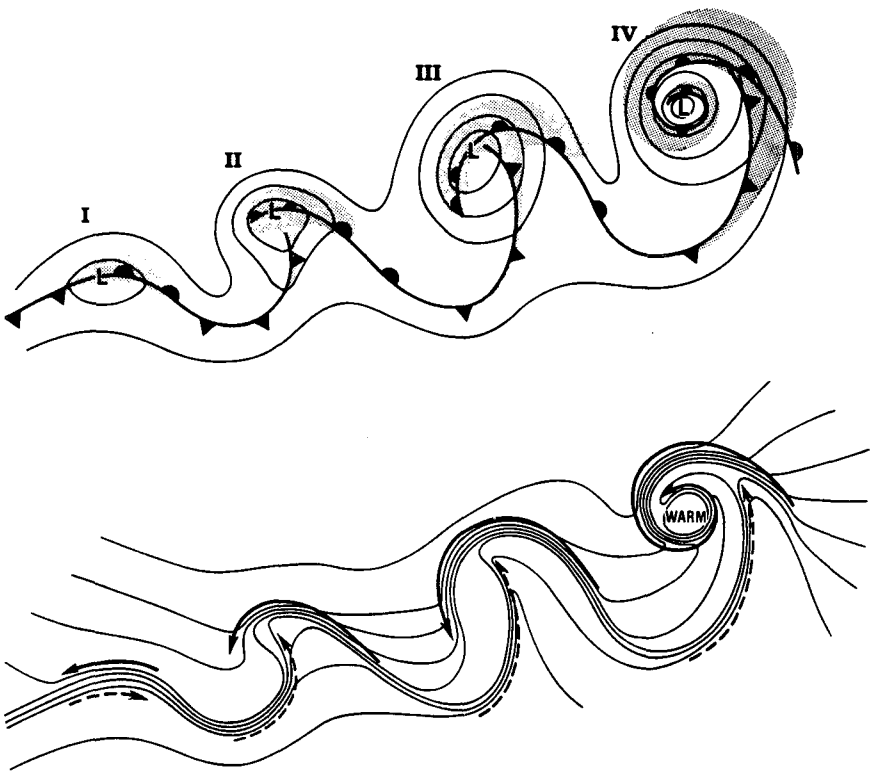

FIG. 7. The life cycle of a marine extratropical frontal cyclone (Shapiro and Keyser 1990). (I) incipient frontal cyclone; (II) frontal fracture; (III) bent-back warm front and frontal T-bone; (IV) warm-core frontal seclusion. Upper panel: sea level isobars, fronts, and cloud signatures. Lower panel: temperature and cold and warm air currents.

• What is the relationship between the structures identified by Shapiro and Keyser (1990) and those of the classical occlusion process? Are such nonideal structures only apparent in marine cyclones?

Considering the lack of certainty of what is meant by the term *occlusion,* an interim working definition will now be stated. The occlusion process is one in which the low center becomes progressively separated from the warm sector of a cyclone. After occlusion, a pressure trough and an associated tongue of intermediate temperature air extends from the low center to the warm sector. This feature, called the occluded front, is generally associated with veering of the surface winds.

3. Model and storm description

This study relied on output from a three-dimensional numerical model simulation of the 14–16 December 1987 storm to document the occlusion process. The simulation employed the Pennsylvania State University–National Center for Atmospheric Research (PSU–NCAR) Mesoscale Model version 4 (MM4) with 16 vertical levels and a horizontal grid resolution of 45 km. The model was initialized at 1200 UTC 14 December 1987 and integrated for 36 h to 0000 UTC 16 December over a domain covering all of the contiguous United States from roughly 20° to 55°N and 125° to 75°W. Further information regarding the simulation can be found in Mass and Schultz (1993).

Although Mass and Schultz (1993) present an overview of the simulated cyclone structure and evolution, a brief summary is given here. At the initialization time (1200 UTC 14 December 1987), there was a broad low pressure region over southern Texas and northern Mexico. As a strong short-wave trough moved into the base of a planetary-scale trough over the central United States, the cyclone center began to deepen and move northward, developing well-defined cold and warm fronts. Cold-air damming on the eastern side of the Appalachian Mountains deformed the warm front. By 24 h into the simulation (1200 UTC 15 December 1987), the surface low center had moved into southern Illinois and deepened to 975 mb. At this time, the model occluded front began to form at the surface as the warm sector air separated from the surface low center. In the next 3 h, the occluded front grew to over 500 km in length. By 36 h into the simulation (0000 UTC 16 December 1987), the surface low center was located in Michigan and the intersection of the cold, warm, and occluded fronts (i.e., the *triple point*) was

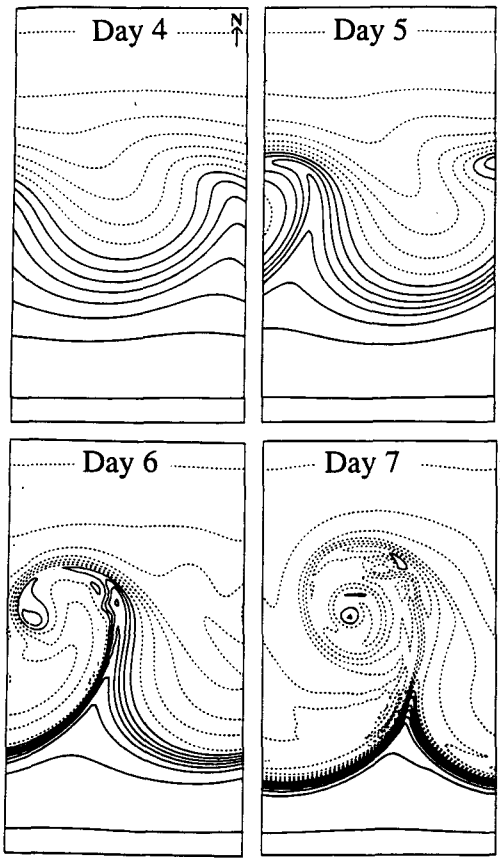

FIG. 8. Surface potential temperature field from a primitive equation simulation of cyclone evolution for days 4, 5, 6, and 7 (Polavarapu and Peltier 1990). The domain is 3142 km × 5500 km, the contour interval is 2 K, and potential temperatures below 0°C are indicated with dashed lines.

in Pennsylvania near a developing secondary low center.

Even though the simulation was generally quite good, there were some minor differences with observations. The most significant discrepancies were the slower than observed motion of the cold front, the resulting delay in occlusion, and an overdeepening of the central pressure.

4. The structure and evolution of the occluded front

A multifaceted description of the simulated structure and development of the occluded front within the 14–16 December 1987 cyclone is presented in this section. First, the vertical structure of the cyclone is examined using cross sections. Second, the airflow near the occluded front is studied using air-parcel trajectories calculated from the model output. Then the movements of the surface warm and cold fronts are considered in light of the classical occlusion mechanism. The fourth subsection examines frontogenesis in the context of the occluded front formation. Finally, surface θ_e maps are presented to show the evolution of the surface thermal structures.

a. Vertical structure

Vertical cross sections were generated before and during occlusion (Fig. 9). At each time, two cross sections intersecting in a V were constructed so that each limb was roughly perpendicular to the relevant frontal zone, with the vertex of the V placed 630 km (14 grid points) away from the low center into the warm sector or (when occluded) along the occluded front. (The positions of the cross sections are shown in Fig. 12 of Mass and Schultz 1993.) The thick solid lines represent thermal gradient discontinuities and should not necessarily be interpreted as Norwegian model frontal boundaries. These subjective analyses were aided by the use of horizontal maps.

At 18 h, an upper-level frontal zone extended downward from the tropopause and approached a surface-based cold front, which tilted forward with height below 800 mb.[6] A mesoscale baroclinic zone represented by heavy dashed lines is noted in the warm sector. This feature, also identified in the observations, was characterized by strong warm advection, saturated conditions, and a vertical velocity maximum. Its origin could not be determined from the model simulation since this feature was present at the time of model initialization (i.e., 1200 UTC 14 December).

By 24 h, the upper-level front appeared to merge with the surface-based cold front. Additionally, the warm sector baroclinic zone had risen over the warm frontal zone. The separation of the upper portion of the warm front into distinct mesoscale baroclinic zones is similar to the "leafed" structure described in Kreitzberg (1964).

At 30 h, the warm- and cold-frontal zones met at low levels in the plane of the cross section, removing the warm-sector air from the surface. Three hours later (33 h), the upper-level frontal zone was further advanced than the surface occluded front, producing a structure reminiscent of a classical warm-type occlusion. Note that the upper front has weakened in this cross section.

To summarize, these cross sections show several important features.

1) The surface-based cold front appeared to catch up to the warm front as in a classical occlusion. Although they appeared to merge at low levels, the cold front did not ride up over the warm front as in the ideal cyclone model.

2) The upper-level frontal zone appeared to overtake and join with the surface-based cold front. In the

[6] This forward tilt appears to be attributed to adiabatic and/or evaporative cooling in the midtroposphere. See Mass and Schultz (1993) for further discussion of this feature.

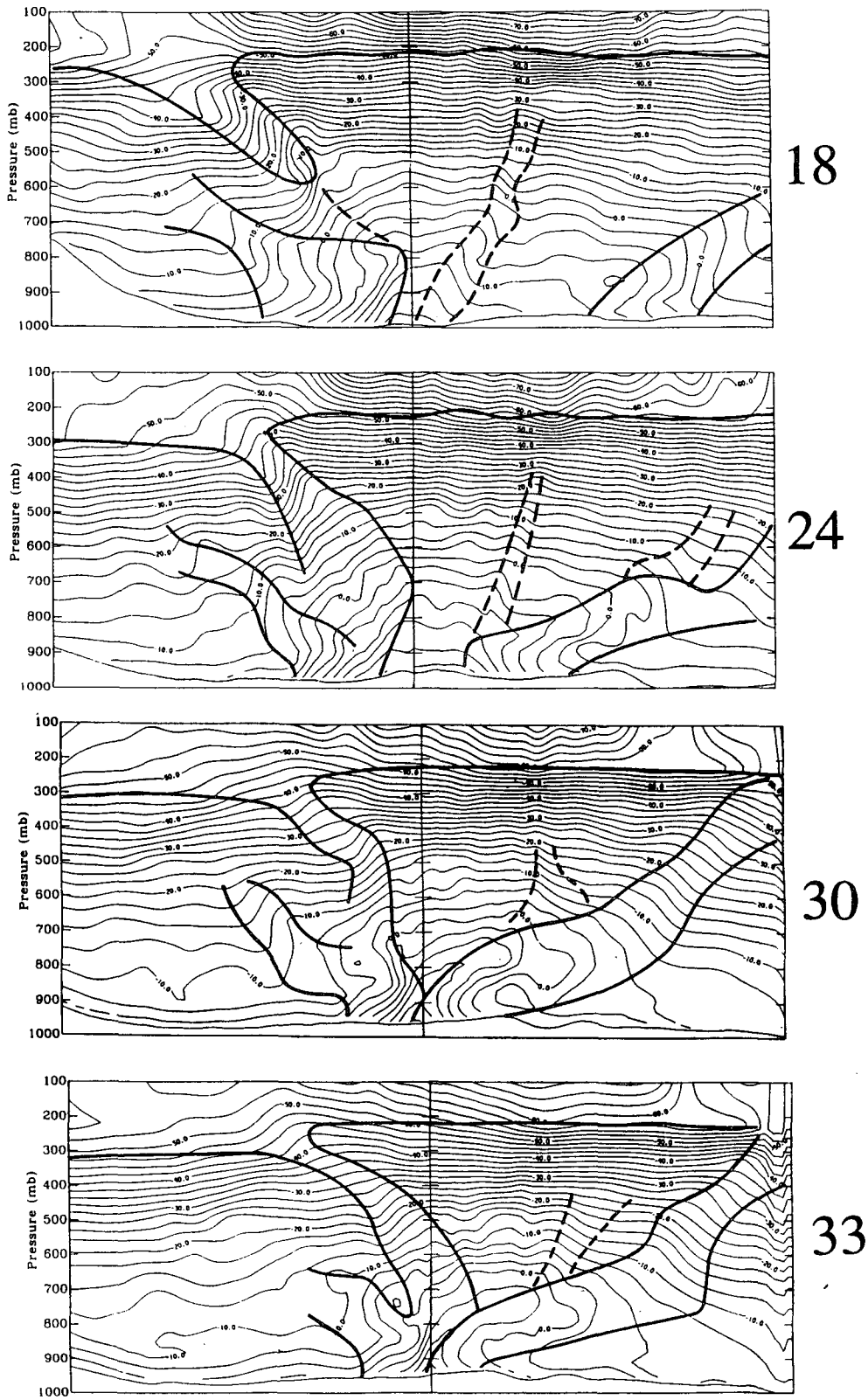

FIG. 9. Vertical cross sections of temperature (thin solid lines) at 18, 24, 30, and 33 h. The contour interval is 2.5°C. Heavy lines represent lines of temperature gradient discontinuities and the tropopause; dashed lines delineate secondary baroclinic zones and the region of temperature gradient between the upper and lower fronts at 18 h. Terrain profile is shown along the bottom of the figure.

later stages, the upper-level front participated in the occlusion process as it appeared to ascend over the surface-based warm front. The resulting structure was reminiscent of a classical warm-type occlusion.

3) A warm-sector baroclinic zone moved faster than the warm front and rode aloft over the warm front.

4) The leading edge of the surface-based cold-frontal zone was either nearly vertical or tipped forward from the surface to as high as 700 mb.

Figure 14 of Mass and Schultz (1993) displays three cross-sectional cuts through the occlusion at 30 h into the simulation. These cross sections illustrate the weakening of low-level temperature gradients between the triple point and the low center, the extension of dry air aloft to the east of the occlusion, and the narrowing and ascent of the warm sector northward along the occluded front. Finally, cross sections across the occluded front, based on observations, were also constructed and analyzed; the structures found in these cross sections were generally consistent with the results of the model simulation.

b. Air-parcel trajectories

Using the approach described in Seaman (1987), three-dimensional air-parcel trajectories were calculated with particular emphasis on the volume of air enclosing the occlusion. These trajectories were calculated from the 15-min model output files using a 15-min time step in the calculations. Such high temporal resolution was necessary in order to ensure the accuracy of the trajectories in this intense, rapidly developing system (Uccellini 1988, personal communication; Whitaker et al. 1988).

1) PARCEL TRAJECTORIES DURING THE OCCLUSION PROCESS

(i) *Before occlusion*

Nine-hour backward trajectories ending at 21 h into the simulation (nominally 0900 UTC 15 December 1987) at $\sigma = 0.995$ (about 4 mb above the surface) on a grid centered over the surface low are displayed in Fig. 10a. The trajectories are shown relative to their position on the earth (not in a storm-relative frame of reference). The surface frontal positions at the initial (dashed) and final (solid) times of the trajectories are also indicated for reference. The pressure elevation of the trajectories are displayed by varying the width of the trajectory path (see inset for scale), and arrowheads along the trajectories represent 3-h intervals.

Two types of trajectories are evident: some originate within the warm sector (e.g., 169, 171, and 189; hereafter identified as *W*) and others, originating north of the surface warm front, move westward or southwestward and rotate around the low center as it moves to the northeast (e.g., 143, 153, and 191; hereafter iden-

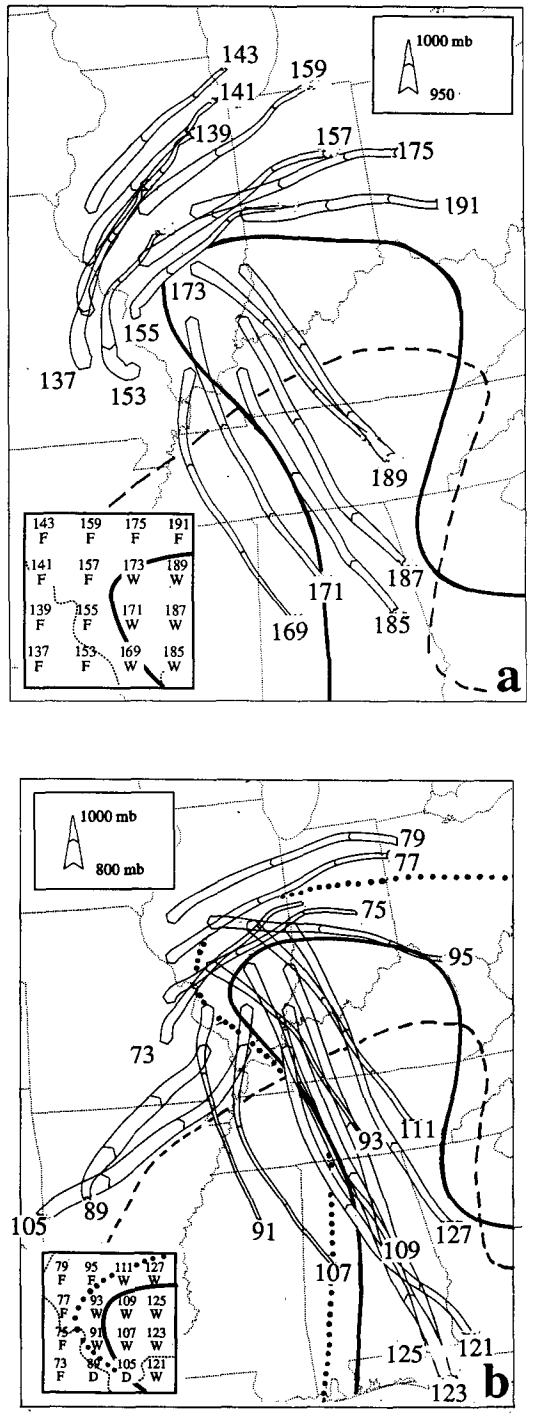

FIG. 10. Nine-hour backward trajectories ending at 21 h (0900 UTC 15 December). (a) Trajectories ending on $\sigma = 0.995$. Solid (dashed) lines represent the 21-h (12-h) surface frontal positions. Inset shows origin of trajectories (*W* represents warm sector trajectory; *D* represents dry, descending trajectory; *F* represents trajectory starting north of the warm-frontal zone; ending positions are centered on the letters). The width of the trajectories are proportional to their pressures (heights) as shown in inset. Arrowheads along the trajectories represent 3-h intervals. (b) Same as (a) except that trajectories end at $\sigma = 0.895$. The boundary between *W* and *F* trajectories are shown by a dotted line.

tified as F). The confluence of trajectories of widely varying origins (and initial temperatures) toward the low center implies substantial frontogenesis. A second inset in Fig. 10a shows the 21-h surface frontal positions overlain on the ending locations of the trajectories, which are identified by their number and type (either W or F). Note that with one exception (169), the front sharply separates trajectory types; W trajectories alone are found in the warm sector, while the F trajectories are limited to the frontal zone.

Trajectory 169 began in the lower troposphere in the warm sector and ended in the cold-frontal zone. Its path may be explained by boundary-layer effects that allow an air parcel to pass through a frontal zone at low levels. Since surface drag near the surface decreases wind speed in the planetary boundary layer, air parcels near the surface are often overtaken by fronts. Several studies on the low-level structure of cold fronts suggest a rather strong front-to-rear flow at low levels (Smith and Reeder 1988). Trajectories above the boundary layer are generally more consistent with the fronts acting as material surfaces.

Nine-hour trajectories (again backwards from 21 h) ending at $\sigma = 0.895$ (about 870 mb), the initial and final surface frontal positions, and the boundary between W and F trajectories (dotted) are shown in Fig. 10b. Besides the two types of trajectories already discussed, there were dry, descending trajectories behind the final cold-front position (89, 105; denoted by a D). The other trajectories at this level generally resemble the trajectories at the $\sigma = 0.995$ level. Note how the warm-sector trajectories (W) extend northward beyond the boundaries of the surface warm sector, consistent with a forward tilt of the warm front.

(ii) *Beginning of occlusion*

Figure 11a shows selected 15-h backward trajectories ending at $\sigma = 0.995$ (about 4 mb above the surface) at 27 h (nominally 1500 UTC 15 December 1987)—a time when the occluded front was evident in the simulation. Trajectories such as 82 and 98 indicate that some of the air that finished near the peak of the warm sector originated within the cold air dammed on the eastern side of the Appalachian Mountains (identified by W' in Fig. 11a). In contrast, the air farther south in the warm sector originated and remained within the warm sector [not shown here but displayed in Fig. 18 of Mass and Schultz (1993)]. The occluded front itself represents a confluence line between easterly flow originating north of the initial warm front and southerly air originating from both the damming region (e.g., 38, 54) and the warm sector (22, 36); thus, the occluded front represents a zone of active frontogenesis as air parcels of substantially different initial temperature are brought together. The frontogenetical nature of the occlusion is further illustrated in Fig. 11b, which presents the 1000-mb temperature field at 12 h into the simulation (the beginning time of the trajectories shown in Fig. 11a) and a limited number of trajectories on both sides of the incipient occlusion.

Figure 11c shows trajectories ending at 27 h at $\sigma = 0.895$ as well as the initial and final surface frontal positions. The trajectories ending at the peak of the warm sector at this time and level originated in the warm sector far to the southeast over the Gulf Stream (e.g., 51). Several F trajectories circled around the low center and ended behind the cold and occluded fronts (e.g., 28, 35). Also note the general separation of the W trajectories from the low center. This contrasts with the preocclusion stage (Fig. 10b), during which a tongue of warm-sector trajectories reached the low center.

Figure 11d illustrates trajectories ending at $\sigma = 0.595$ (about 615 mb). At this level, the cyclone had an open wave structure with warm-sector trajectories terminating north of the surface occluded front all the way to the low center (e.g., 13, 22). Over much of the occluded front, dry descended trajectories (e.g., 21, 29) are noted. Also note the distinct difference between the paths of trajectories 13 and 22, which start in the northern part of the warm sector and move northwestward into the low center, and trajectories 43 and 51, which began deeper in the warm air and headed off to the northeast. Some trajectories (e.g., 19, indicated by M) remain in the midtroposphere and evince little vertical motion [similar to Whitaker et al.'s (1988) cyclical trajectories].

(iii) *Mature occlusion stage*

At 33 h (Fig. 12), the trajectory pattern at $\sigma = 0.995$ is similar to that at 27 h, with the occluded front associated with a confluence of trajectories. On the northern side of the occluded front, the trajectory origins varied from deep within the cold air (8) to within the warm frontal zone (43). Behind the occluded front, some trajectories (6, 24, and 39) began in the warm sector (passing through the cold front in the interim), and others (49) had descended from aloft. Trajectories 55–57 (56 not shown) started in the cool, easterly flow to the east of the Appalachians and entered the warm sector before passing through the cold-frontal surface and ending behind the cold front. Considering the varied temperatures of the source regions of the air parcels converging toward the occluded front, the later feature continues to represent an area of active frontogenesis.

At $\sigma = 0.895$ (not shown), the trajectories are similar to those of the lower level; however, at this level, warm-sector trajectories from deep within the warm air extended over the southern sections of the occluded front and far fewer trajectories originating within the warm sector were found behind the occluded front.

At $\sigma = 0.595$ (Fig. 12b), warm-sector trajectories (e.g., 35, 38, and 46) ascended to the northeast of the surface occluded front, while trajectories originating in the easterly flow north of the initial warm front (e.g., 9, 10) circled around the low center as they rose vig-

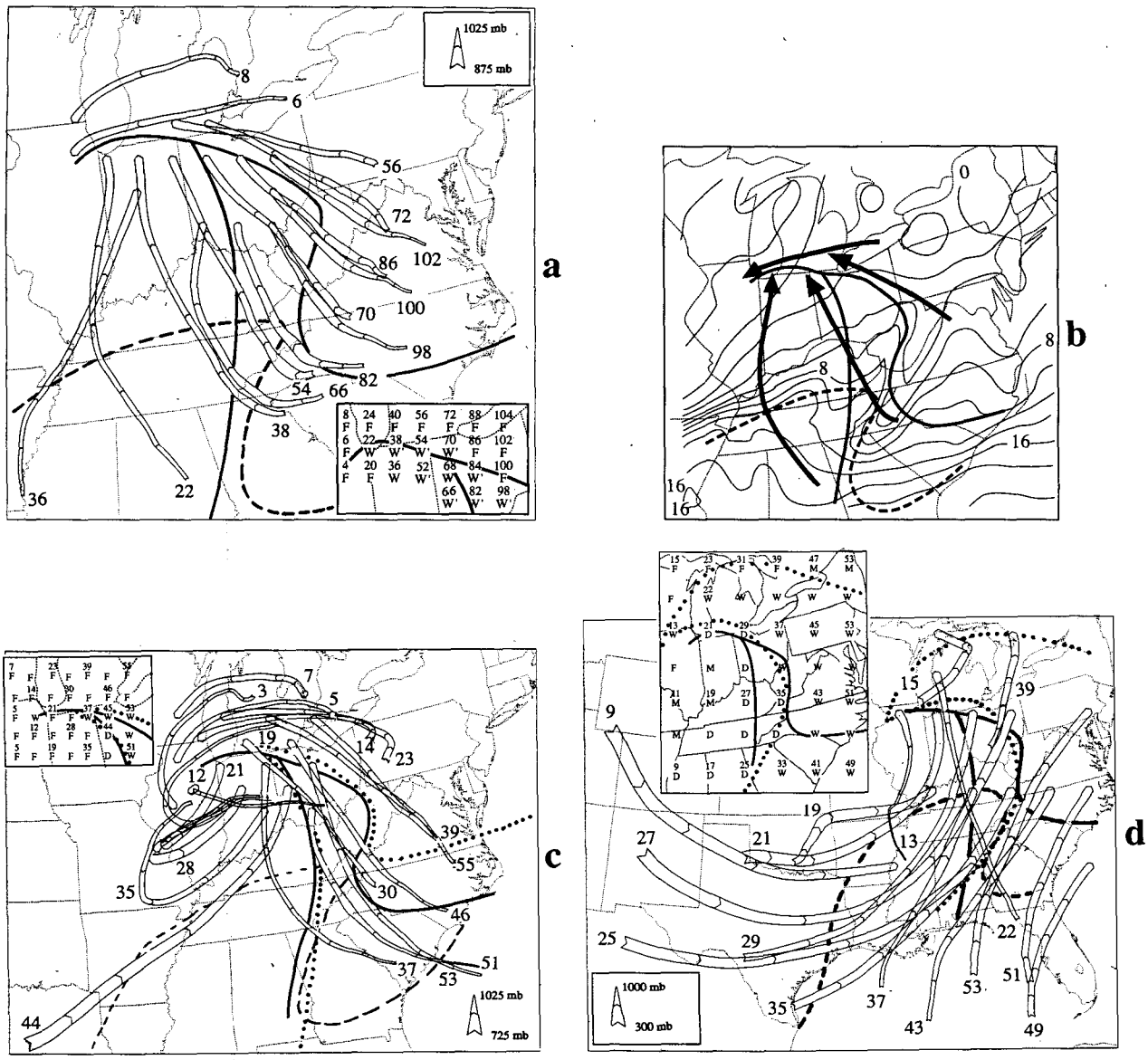

FIG. 11. (a) Fifteen-hour backward trajectories ending at 27 h and $\sigma = 0.995$. Notation as in Fig. 10. (b) The 1000-mb surface temperature field at 12 h into the simulation (nominally 0000 UTC 15 December 1987). Some selected trajectories from (a) are also shown. (c) Trajectories ending at $\sigma = 0.895$. (d) Trajectories ending at $\sigma = 0.595$. Letter *M* represents midtropospheric flow trajectories.

orously to positions north and west of the occluded front. These warm frontal trajectories are crossed by subsided trajectories (e.g., 23), which initially descended from the midtroposphere and later began to rise, finishing behind, over, and ahead of the surface the occluded front.

2) Analysis of trajectories along a cross section across the occluded front

A temperature cross section perpendicular to the surface occluded front at 33 h (Fig. 13a) was constructed along section *AB* shown in Fig. 13b. The numbered dots in Fig. 13a indicate the final locations of 21-h backward trajectories ending within the cross section at 33 h. There is no distinct back edge to the upper front analyzed in Fig. 13a since cross section *AB* was nearly parallel to the baroclinic zone at 500 mb.

The 33–12-h trajectories ending at the lowest level ($\sigma = 0.995$), shown in Fig. 13b, indicate a distinct break in the nature of the trajectories across the occluded front. Trajectories 1, 8, and 15 all approached the occluded front from the west, with trajectory 1 originating in the cold northerly flow behind the cyclone; trajectory 8 starting out in the warm sector, passing into the cold-frontal zone, and ending up in the occluded frontal zone; and trajectory 15 being part of the dry, descended airstream. In contrast, trajectories 22, 29, and 36 began within the cold anticyclone in

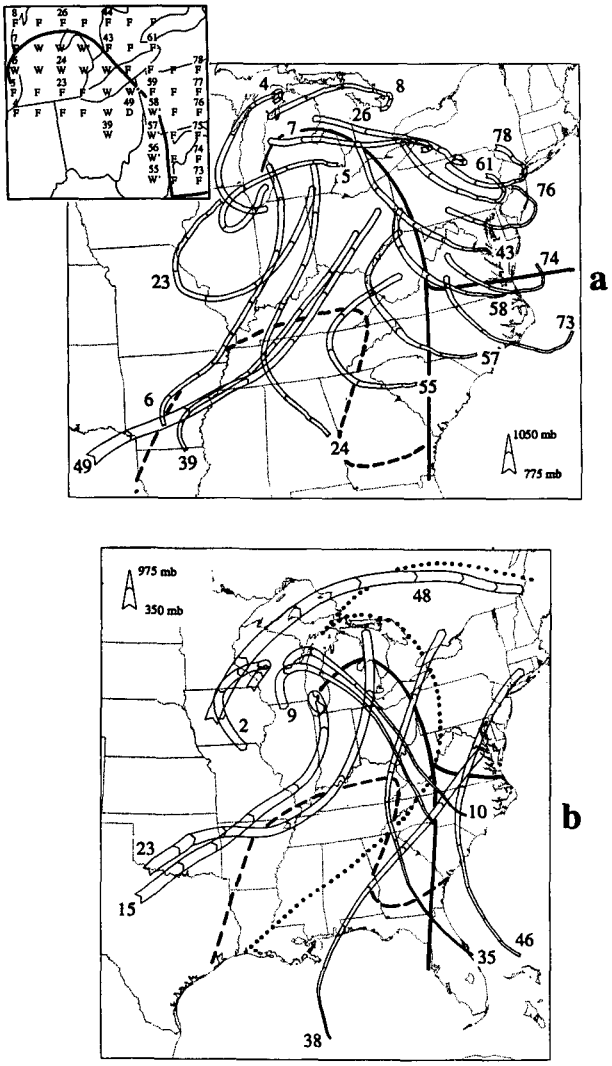

FIG. 12. Twenty-one-hour backward trajectories ending at 33 h. Notation as in Fig. 10 except that W' represents warm-sector trajectories that start out in the dammed cold air. (a) Trajectories ending at $\sigma = 0.995$. (b) Trajectories ending at $\sigma = 0.595$.

advance of the cyclone and approached the occlusion from the east. These results highlight the great kinematic significance of the occluded front—it serves as a boundary between two air masses with distinctly different sources.

Air-parcel trajectories ending within the cross section at $\sigma = 0.795$ are found in Fig. 13c. Trajectories 3 (not shown), 10 (not shown), and 17 originated within the warm-frontal zone, ascended behind the low center, and then descended into the surface-based cold-frontal zone. Trajectory 24 descended from nearly 650 mb to behind the occluded front before rising again as it neared the low center. In contrast, trajectories 31 and 38 started at low levels on the warm boundary of the lower-tropospheric baroclinic zone and ended in the warm air core of the occluded front. Trajectory 45 descended until it was caught in the ascending W flow along the warm-frontal surface and turned northward.

Trajectories ending at $\sigma = 0.655$ (~675 mb) are shown in Fig. 13d. Trajectory 5 started in the warm-frontal zone, ascended as it circled around the low center, and ended within the upper sections of the surface-based cold-frontal zone. Trajectories 26 and 33 (not shown) were in the dry, descended airflow. Trajectories 40 and 47 originated deep within the warm sector near the surface and finished in the warm tongue aloft. Trajectory 61, a midtropospheric trajectory, moved northeastward with relatively little vertical motion.

Trajectories ending at $\sigma = 0.495$ (about 530 mb) are shown in Fig. 13e. Trajectories 21 and 28 belonged to the dry, descended air stream that ended behind the upper-level front. Trajectories 42 and 56 were warm-sector trajectories that had ascended the warm front. Trajectory 70 was midtropospheric air with relatively little vertical motion.

3) SUMMARY OF TRAJECTORIES

By studying the trajectories in the simulated cyclone, several interesting results were obtained.

1) The occluded front in the lower troposphere was a significant kinematic entity representing the boundary between different airstreams.

2) Considering the varied thermal origins of the confluent lower-tropospheric trajectories approaching the occluded front, it is clear that the occluded front is a zone of active frontogenesis.

3) The tongue of warm air aloft of the occlusion was composed of air that originated in the warm sector (W).

4) Trajectories show that the warm-sector air (W) was removed from the lower troposphere as the occlusion progressed in time.

c. *Frontal movement*

To form an occluded front through the ideal Bergen school mechanism (i.e., a cold front overtaking a warm front), the component of the cold-frontal velocity *in the direction of the warm-frontal movement* must be greater than the speed of the warm front near the point of occlusion. In the model simulation just before occlusion began, the surface cold front moved at a speed of 46 km h^{-1} in the direction of the warm-frontal movement, while the warm front moved at a speed of 30 km h^{-1}. These results are consistent with the cold front catching up to the warm front as in an ideal occlusion. Frontal movement rates at 800 mb in both the model and observations verified that the cold front was moving faster than the warm front not only at the surface but aloft as well.

d. *Frontogenesis*

The nature of the occlusion process can also be studied by examining the distribution of frontogenesis near

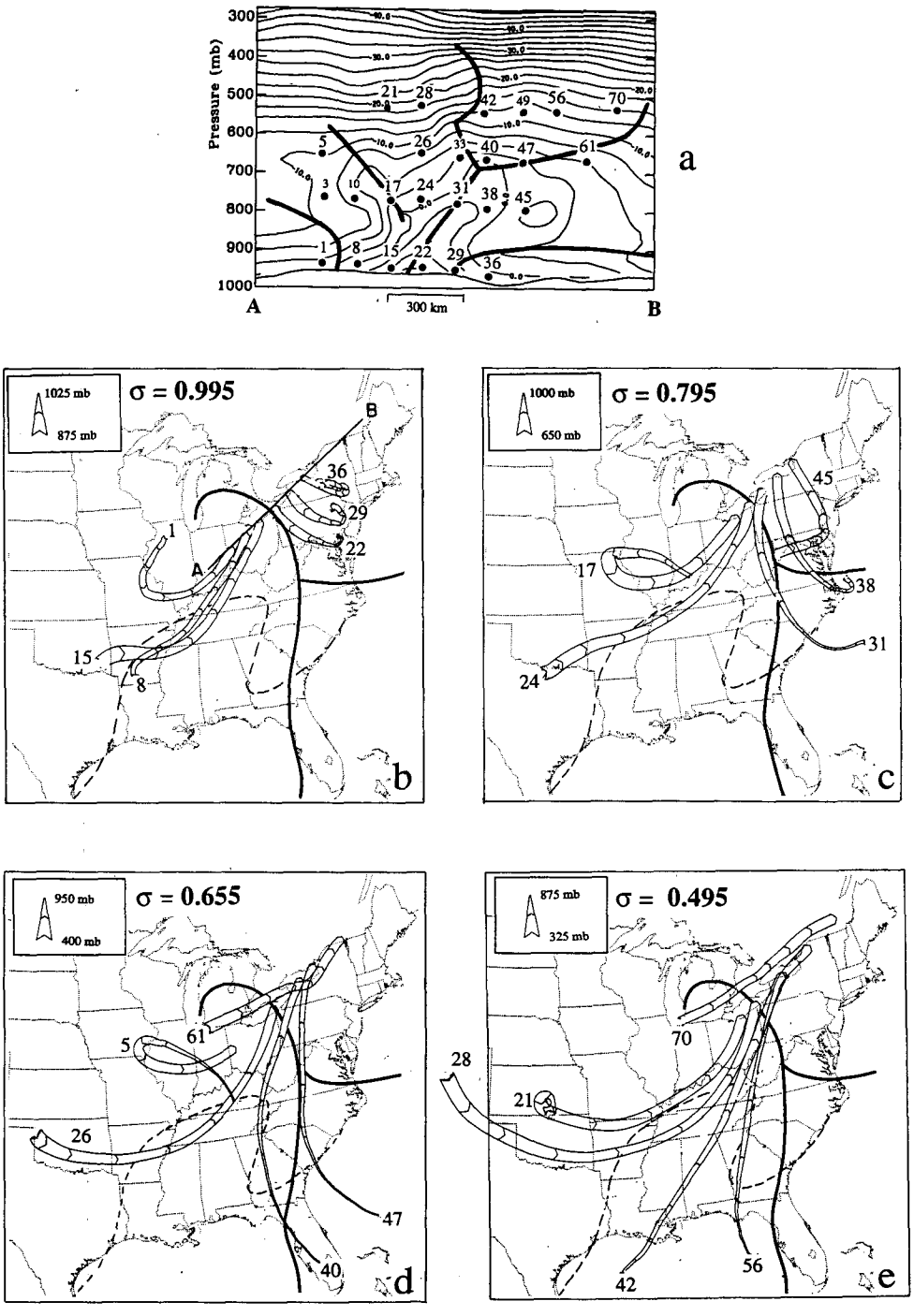

FIG. 13. (a) Vertical cross section *AB* at 33 h showing locations of trajectories depicted in (b)–(e). Temperature presented using 2.5°C contour intervals (solid); heavy lines represent temperature gradient discontinuities. Numbered dots represent ending locations of trajectories. (b)–(e) 21-h backward trajectories ending at 33 h along the cross section in (a). Dashed (solid) lines represent surface frontal positions at 12 (33) h into the simulation. (b) Trajectories ending at $\sigma = 0.995$. Line *AB* depicts the location of cross section *AB* in (a). (c) Trajectories ending at $\sigma = 0.795$. (d) Trajectories ending at $\sigma = 0.655$. (e) Trajectories ending at $\sigma = 0.495$.

the surface. For example, the development of a new area of frontogenesis into the cold air during cyclone development might support the contention of Wallace and Hobbs (1977) that "occluded fronts are essentially new fronts which form as surface lows separate themselves from the junctions of their respective warm and

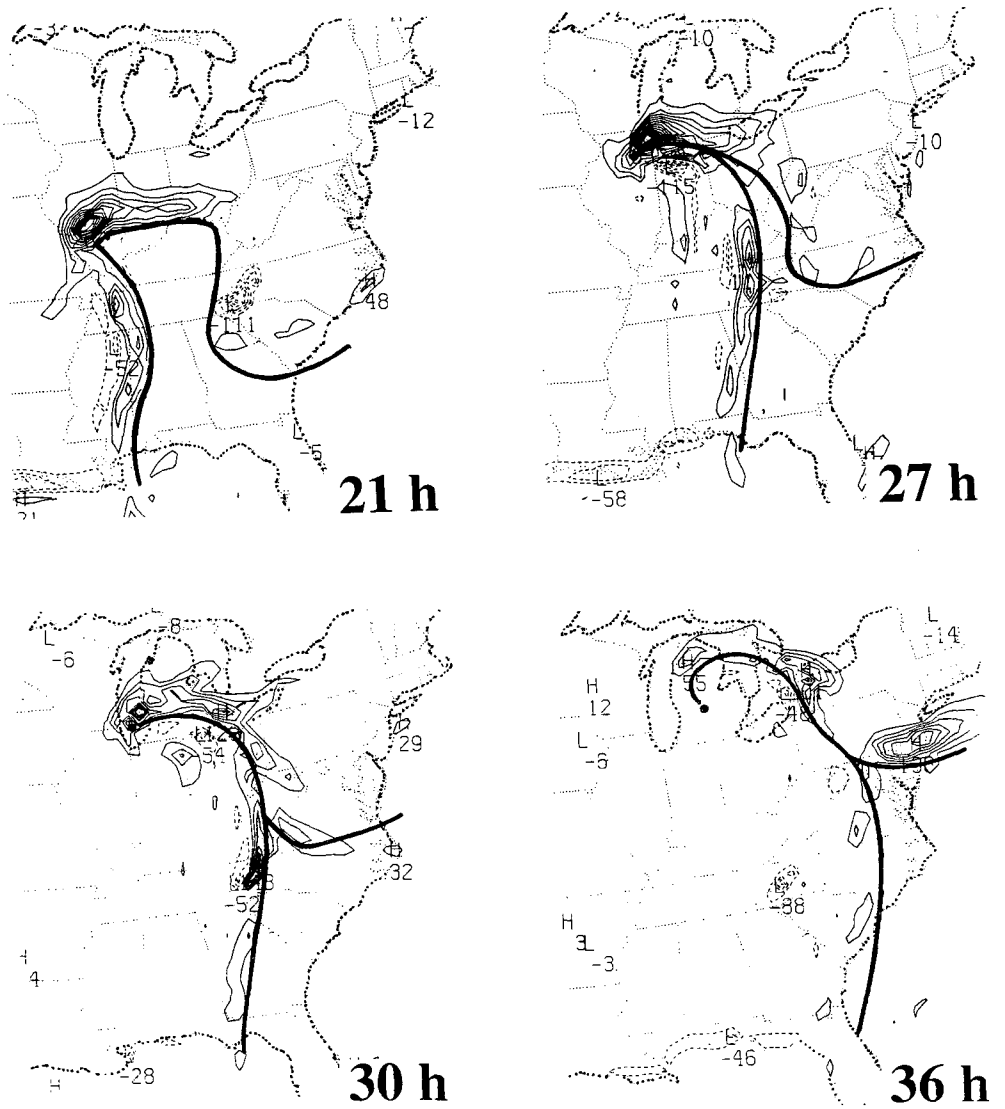

FIG. 14. Surface frontogenesis at 21, 27, 30, and 36 h into the simulation. Contour interval is 0.2×10^{-8} K m^{-1} s^{-1} or approximately 2°C (100 km)$^{-1}$ (3 h)$^{-1}$. Model surface frontal positions are also shown. Maximum values of the frontogenesis at each time are 2.62, 3.32, 1.48, and 1.38×10^{-8} K m^{-1} s^{-1}.

cold fronts and deepen progressively further back into the cold air." On the other hand, a surface frontogenesis pattern showing separate cold and warm frontogenesis regions merging into one would be consistent with the ideal cyclone model in which the cold front meets the warm front to form an occlusion.

Figure 14 presents surface frontogenesis, based on model fields at 21, 27, 30, and 36 h, that were calculated using the approach of Miller (1948).[7] At 21 h, the most pronounced features were the frontogenetical regions supporting the cold and warm fronts. Maximum surface frontogenesis occurred along the warm front, especially in the vicinity of the low center. As shown in the trajectory section, this region was one of significant confluence of air parcels with a wide range of original temperatures. Frontogenesis was less intense along the northern section of the cold front. At 27 h, the frontogenesis along the northern part of the cold front continued to weaken; intriguingly, the frontogenesis distribution at this time is suggestive of the (cold-) frontal fracture described by Shapiro and Keyser (1990) and Donall et al. (1991). *It appears that a single frontogenesis feature supports both the warm and occluded fronts.* The strong frontogenesis at the surface along the length of the occluded front at 30 h belies any notion that occluded fronts are inherently weak

[7] See Mass and Schultz (1993) for the frontogenesis fields at other times and for more information on the frontogenesis calculation.

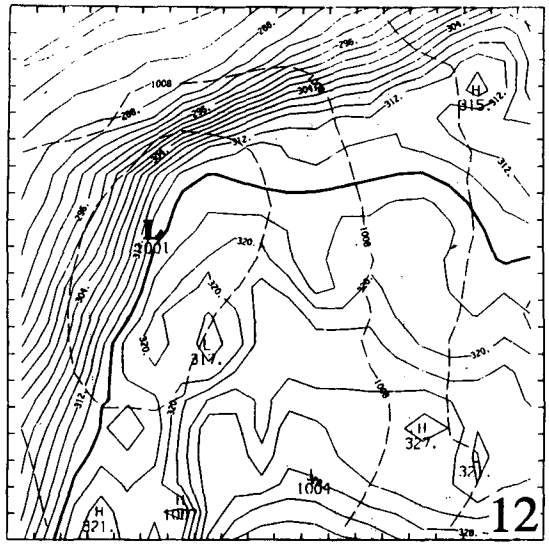
12

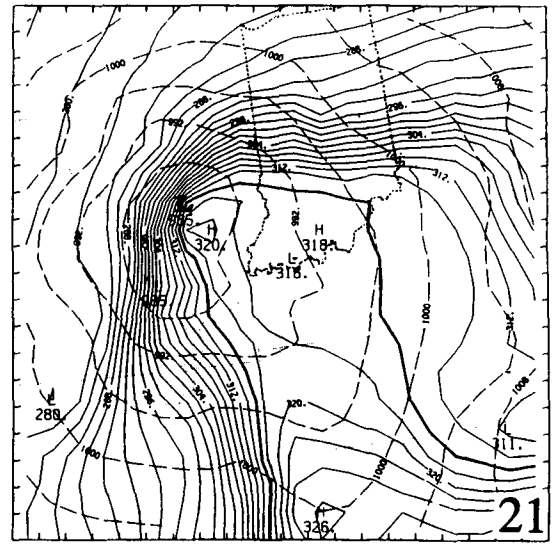
21

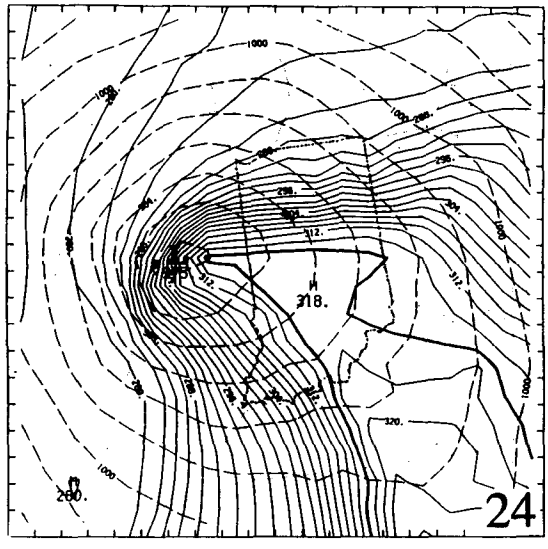
24

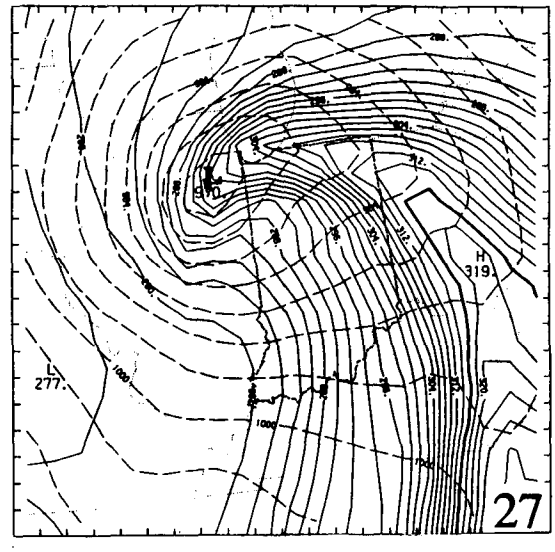
27

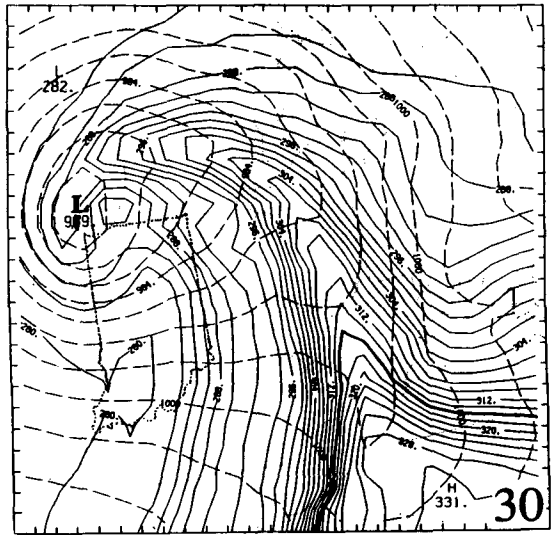
30

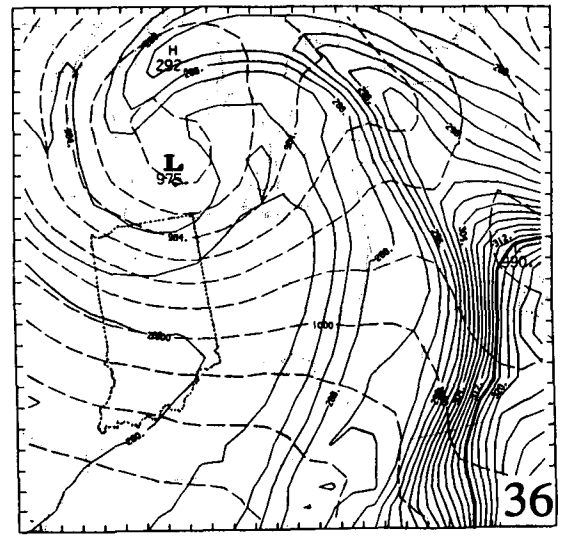
36

and dynamically inactive (e.g., Postma 1948; Saucier 1955). Frontogenesis along the cold front is very weak at this time. Finally, at 36 h, frontogenesis along the occluded front had attenuated and the warm frontogenesis began to increase greatly in magnitude with the formation of the secondary low center near the triple point.

e. *Equivalent potential temperature*

In the absence of processes such as mixing, ice microphysics, moisture fluxes, or diabatic heating, equivalent potential temperature θ_e can be used as a tracer for air motions. Calculations presented in Schultz (1990) showed that the effects of mixing, ice microphysics, and latent and sensible heating in the northern portion of the warm sector of the 14–16 December 1987 cyclone could lower the θ_e along an air-parcel trajectory near the surface by no more than 2 K during a 3-h period. An examination of trajectories in the warm sector showed that θ_e changed very little, thereby confirming its conservation. Assuming θ_e conservation, a larger decrease in θ_e near the surface during the occlusion process would suggest that ascending warm-sector air was being replaced by cooler frontal-zone air.

A series of maps of θ_e at $\sigma = 0.995$ (about 4 mb above the surface) near the cyclone center from 12 to 36 h is shown in Fig. 15. Note that throughout the simulation, a θ_e of 316 ± 2 K appeared to coincide with the peak of the warm sector and can be considered as an approximate boundary between warm and transitional air in the frontal zones. Equivalent potential temperature θ_e at the low center progressively decreased during the evolution of the cyclone. For example, at 24 h, the 308-K isotherm extended into the cyclone center, compared with 316 K 3 h earlier. At 27 h, the θ_e at the low center dropped another 10 K to 298 K.

The air in the peak of the warm sector over southern Indiana at 24 h had a θ_e of 317 K. Since the near-surface air-parcel trajectories were towards the north, the air near the surface in the warm sector in southern Indiana would have been advected into northern Indiana at 27 h; thus, one would have expected the air in northern Indiana to have had a θ_e of approximately 317 K and not the actual value of 308 K. These changes in θ_e were too rapid to be explained by any of the nonconservative processes listed above and must therefore be the result of the ascent of near-surface warm air as the cold front approached the warm front. One also notes the progressive temporal weakening of the θ_e gradient associated with the occluded front from 27 through 36 h [consistent with Kreitzberg's (1964) comparison between old and new occlusions].

5. Discussion

Using a variety of approaches, the structure and evolution of the occluded front that developed during the 14–16 December 1987 cyclone were studied using a mesoscale numerical model. A brief summary of the results follows.

Structure. Using vertical cross sections, the development of a structure reminiscent of an ideal warm-type occlusion was documented. Near the surface, this structure appeared to form from the union of the cold- and warm-frontal zones as in the classical model but without the cold front riding aloft over the warm front. Aloft, an upper-level frontal zone that extended from the tropopause participated in the occlusion process. A baroclinic zone in the warm sector appeared to ascend the warm front.

Trajectories. The occluded front was shown to be kinematically significant because it represented a line of confluence of air from different source regions. Even on the same side of the occlusion (e.g., the northern one) there was a confluence of trajectories from regions of widely varying temperature. Trajectory analysis showed that the air that ended in the occlusion's warm tongue aloft originated in the warm sector. The removal of warm-sector trajectories near the surface in the region where the occluded front was forming was consistent with the ideal occlusion process.

Frontal movement rates. The rate at which the cold front traveled in the direction of the warm-front movement was greater than the speed of the warm front, consistent with the cold front catching up to the warm front.

Frontogenesis. Surface-frontogenesis diagnostics illustrated the predominance of the model frontogenesis along the warm and occluded fronts in what appeared to be a single feature. The development of a weakness in the frontogenesis along the northern cold front is reminiscent of the fracturing of the surface cold front described by Shapiro and Keyser (1990).

Equivalent potential temperature. It was shown that the equivalent potential temperature θ_e of the air reaching the low center near the surface decreased during the lifetime of the storm. Assuming that θ_e is nearly conserved in the warm sector of the cyclone (demonstrated in Schultz 1990), this decrease in θ_e must have been due to the ascent of air away from the surface accompanying the meeting of the warm and cold fronts.

a. *Mesoscale features in occluding cyclones*

Kreitzberg (1964, 1968) and Kreitzberg and Brown (1970) showed that the mesoscale structure of occluding cyclones was much more complex than envisioned

FIG. 15. Surface θ_e (solid) and sea level pressure (dashed) maps at 12, 21, 24, 27, 30, and 36 h into the simulation. Contour intervals are 2 K and 4 mb. The 316-K θ_e contour is indicated by a bold solid line. The border of Indiana is highlighted.

in the ideal cyclone model. Since then, many others have documented the existence of these mesoscale features (e.g., Elliott and Hovind 1965; Hobbs et al. 1975; Matkovski and Shakina 1982; Saarikivi and Puhakka 1990). The simulation of the December 1987 cyclone possessed many of the nonclassical features described in these studies.

For example, as shown in Fig. 9, a warm-sector baroclinic zone that extended from the surface to the upper troposphere started out in the warm sector and then rode aloft over the warm front. The structure of this feature was similar to one of Kreitzberg's (1968) warm tongues, being accompanied by strong warm advection and upward vertical velocities. Browning et al. (1973) and Saarikivi and Puhakka (1990) found that the rate of propagation of these warm tongues was faster than the speed of the warm front, and thus they were able to ascend the warm front. As mentioned previously, the origin of the warm-sector baroclinic zone was not clarified in this numerical study since the feature already existed at the time of model initialization.

As described in Mass and Schultz (1993), a feature termed the upper-level humidity front was observed in this cyclone. The fields of moist static energy[8] h and vertical motion in Kreitzberg's (1968) prefrontal surge were similar to those associated with the upper-level humidity front in the model simulation. In this simulation, the humidity front was located between 250 and 1000 km ahead of the upper-level front; Kreitzberg (1968) shows the prefrontal surge 500 km ahead of the primary front. Although Kreitzberg (1968) does not present individually the temperature field and relative humidity fields, he does mention that the air is much drier behind the prefrontal surge. This information suggests rather strongly that the prefrontal surge and the upper-level humidity front are the same. Kreitzberg and Brown's (1970) hypothesis that the prefrontal surge was at one time the primary front and had overrun the lower-level frontal zone and had gone aloft was not verified in this simulation. As discussed in Mass and Schultz (1993), the upper-level humidity front appears to be the same as Browning and Monk's (1982) upper-cold front in their split-cold-front model.

The upper-level front (*not* the upper-level humidity front) in the model simulation and the primary front of Kreitzberg and Brown (1970) appear to be identical features. In the simulation, the upper-level front was preceded by ascending motion of previously descended air, with descending motion within the frontal zone. Kreitzberg and Brown found similar results for their primary front. Kreitzberg and Brown documented an enhancement of the precipitation associated with two structures of the occlusion—one associated with the prefrontal surge and the other with the primary front.

b. *The role of the upper-level frontal zone in the occlusion process*

As shown in section 4, the occluded front developed from the meeting of a surface–upper-level frontal complex and the warm front (Fig. 9). As shown in this figure, the occluded front first formed at the surface as the surface-based cold front met the warm front. Subsequently, the upper-level front participated in the occlusion process by supplying what would traditionally be called the elevated cold front of the occlusion.[9] As discussed in the next subsection, the participation of the upper front in the occlusion process may explain the predominance of warm-type occlusions.

One might speculate that in some cyclones the upper-level front might not descend far enough to meet the warm front, and thus the occlusion process would only be associated with the merger of the lower-tropospheric cold and warm fronts. Furthermore, because the upper level front is often of a smaller horizontal scale than the lower-tropospheric baroclinic zone (see Mass and Schultz 1993), part of the surface-based occlusion may not have an upper-level frontal structure aloft.

c. *The formation of warm- and cold-type occlusions*

As shown earlier (e.g., Fig. 9), the occluded front structure of the 14–16 December 1987 cyclone resembled the warm-type occlusion described by Bjerknes and Solberg (1922) and Bergeron (1937). Bjerknes and Solberg suggested that the type of occlusion depended on the relative temperature of the air masses on each side of the occluded front. In an ideal warm-type (cold-type) occlusion, the air preceding the warm front is colder (warmer) than the air behind the cold front, so that the cold (warm) front rides aloft over the warm (cold) front.

In the 14–16 December case, the air behind the cold front was colder than the air in advance of the warm front throughout the lower troposphere. For example, Figs. 1–3 of Mass and Schultz (1993) show that the air ahead of the warm front was 3°–5°C warmer than found at the same level and distance behind the cold front. Given this information, the ideal occlusion model would predict that a cold-type occlusion would form, in contrast to the simulated (and observed) warm-type occlusion structure.

Bjerknes and Solberg (1922), Saucier (1955), and Petterssen (1956) suggested that cold-type occlusions would be more common than warm-type occlusions since the air to the rear of the cyclone would have come from the polar regions more recently (and thus be colder) than the air ahead of the warm front. When examining the literature on occluded fronts, however, a conspicuous lack of cold-type occlusions was appar-

[8] Moist static energy is $h = gz + c_pT + Lq_v$. Moist static energy, like θ_e and θ_w, is conserved during pseudoadiabatic processes.

[9] The upper-level front in this case cannot correctly be called an upper *cold* front since at some times it can be characterized by warm advection. Keyser and Shapiro (1986) showed that upper-level frontal zones can be associated with warm advection late in their evolution.

ent. Of 21 case studies describing the vertical structure of an occluded front (see the Appendix), only three claimed to have found cold-type occlusion structures.[10] One of these cold-type occlusions could be reanalyzed as a warm-type occlusion (Matejka 1980), another is merely a schematic and does not show any observed data (Elliott 1958), and the other has no well-developed warm frontal zone (Hobbs et al. 1975). The Appendix indicates that there is little correlation between the character of the temperature contrast across an occlusion and its structural type (i.e., warm- or cold-type occlusion).

This absence of a well-documented cold-type occlusion may be related to the differential propagation speed of the upper- and lower-level fronts. As shown in this case and amply discussed in the literature (e.g., Browning 1990), dry airstreams aloft and upper-level fronts tend to advance faster than the surface cold fronts. Thus, the general tendency is for upper-level fronts to advance over the warm front more rapidly than the surface cold front, thereby forming what appears to be a warm-type occlusion. This is consistent with the tendency for the baroclinic wave to become vertically stacked as the occlusion process progresses. Since this phasing between upper- and lower-level fronts appears to be a frequent, if not a general, feature of cyclone evolution, one would expect that warm-type occlusions would predominate; *cold-type occlusion structures, if they exist at all, may not be able to persist throughout the mature stage of a cyclone's life cycle.*

d. The nature of the occlusion process

The detailed diagnosis of the simulated occlusion process of the 14–16 December 1987 storm displayed both consistencies and contradictions with the classical Norwegian cyclone model. Consistent with the classic paradigm [and in variance with some new models of cyclone evolution—e.g., Shapiro and Keyser (1990)], it was found that

1) the cold front caught up with the warm front to form an occlusion at low levels;
2) there was little evidence of significant fracturing of the temperature field in the northern section of the cold front;
3) a relatively classic occlusion structure formed, with little evidence of a bent-back warm front; and
4) no evidence of a warm-core seclusion was apparent near the surface.

On the other hand, there were a number of inconsistencies with the Bergen school paradigm:

1) a warm-type occlusion formed even though the cyclone's temperature structure suggested that a cold occlusion should be expected;
2) an upper-level front (distinct from the surface-based cold front) contributed to the warm-type occlusion that has traditionally been called the elevated cold front; and
3) frontogenesis was most intense along the warm and occluded fronts, with frontogenesis along the cold front being substantially weakened along its northern section—this frontogenesis pattern is reminiscent of the Shapiro and Keyser conceptual model in which frontogenesis along the warm front dominates.

The central question regarding the origin of occluded fronts is whether they 1) form as a cold front catches up to a warm front (the traditional Norwegian conceptual model), 2) are essentially new fronts that form as the low center propagates into the cold air (Wallace and Hobbs 1977), 3) form in other yet undiscovered ways, or 4) do not exist at all (Keyser and Shapiro 1990). Although there appears to be little question that the cold front caught up with the warm front during the simulated December 1987 event, this does not necessarily prove that other processes might not have contributed to the development of the occluded front or that the catch-up mechanism is essential to the occlusion process (as implied in the Norwegian model). Numerous primitive equation simulations (e.g., Takyabu 1986; Keyser et al. 1989) have produced occluded structures (with a narrow tongue of warm air circling into a low center) with apparently no overtaking of warm fronts by cold fronts. In these simulations, the tongue of warm-sector air appears to narrow in time, giving the appearance of occlusion, but without the classic catch-up process. This is not to say that the "catch-up" process cannot occur, but rather that it may not be only mechanism associated with the occlusion process in midlatitude cyclones.

It is also important to stress that the occluded front in the model simulation was a region of active frontogenesis. This fact was clearly indicated not only by the surface frontogenesis diagnoses presented in section 4d but by the confluence of trajectories from widely varying source regions described in section 4b. The contribution of the frontogenesis associated with the cold front was quite small and the frontogenesis supporting the occlusion was indistinguishable from that of the warm front.

A significant challenge is to determine the conditions conducive to the various types of occlusion evolution. Recent work by Hines and Mechoso (1992, personal communication) suggest that increasing amounts of surface drag in baroclinic channel models favor the formation of structures similar to those of the classical occluded-front structure, whereas experiments conducted with oceanic values of friction led to the formation of structures more reminiscent of the Shapiro and Keyser model, with a back-bent warm front replacing the occlusion.

[10] If occluded-like structures like Locatelli et al.'s (1989) are also included, this suggests that this slanting-forward structure may be favored in cyclones regardless of the process of formation.

6. Summary

This paper reviews the literature regarding occluded front structure and development and appraises the validity of the ideal occlusion model for an explosively deepening continental cyclone. The examination of this cyclone made use of a dataset produced by a PSU–NCAR Mesoscale Model version 4. The main conclusions of this paper are as follows.

- The model simulation produced a warm-type occlusion structure. Near the surface, the occluded structure formed from the union of the cold and warm frontal zones as in the classical model, while aloft an upper-level frontal zone that extended from the tropopause contributed what is normally termed the elevated cold front of the occlusion. The surface-based cold front did not ride aloft over the warm front as in the ideal cyclone model.
- The occluded front was shown to be kinematically significant, with different source regions for the air on either side. Even on the same side of the occlusion (e.g., the northern one), there is a confluence of trajectories from regions of widely varying temperatures. Trajectory analysis showed that the air that ended in the occlusion's warm tongue aloft originated in the warm sector.
- At the surface, the rate at which the cold front traveled in the direction of warm-front movement was greater than the warm-front speed and thus was consistent with the cold front catching up to the warm front.
- A single region of surface frontogenesis was found to support both the warm and occluded fronts. A weakness in the frontogenesis along the northern portion of the surface cold front suggested the existence of the frontal fracture described by Shapiro and Keyser (1990), although the temperature field did not show this break.
- It was shown that the θ_e of the air reaching the low center decreased during the lifetime of the storm. Assuming θ_e to be nearly conserved for air parcels within the warm sector of the cyclone, the decrease in θ_e near the low center must have been due to the removal of air from near the surface accompanying the meeting of the warm and cold fronts.
- A warm-sector baroclinic zone, resembling one of Kreitzberg's (1968) warm tongues, originated in the warm sector and propagated up along the warm-frontal surface. Kreitzberg's prefrontal surge was similar to the simulated upper-level humidity front, and his primary front resembled the upper-level front of this simulation.
- The lack of well-documented cases of cold-type occlusions in the literature suggests that cold-type occlusions may not exist in a mature cyclone, with warm-type occlusions being the normal structural form. The thermal contrast across the occluded front did not appear to affect the type of occluded structure that formed (warm type or cold type).
- The detailed diagnosis of the simulated occlusion process of the 14–16 December 1987 storm displayed both consistencies and contradictions with the classical Norwegian cyclone and more recent (e.g., Shapiro and Keyser 1990) models of cyclone evolution.

Acknowledgments. Dr. Ying-Hwa Kuo and Dr. Richard Reed made possible our acquisition of the model data used in this research. This work was funded by the National Science Foundation under Grant ATM-8912472. The mesoscale model was run by Dr. Georg Grell at the Scientific Computing Division at the National Center for Atmospheric Research, which is sponsored by the National Science Foundation. Dr. Grell was supported by the Office of Naval Research (Grant N00014-90-J-1208). Mark Stoelinga and Yea-Ching Tung helped with the display of the trajectories. Profs. Richard Reed and Dale Durran, Jon Martin, Mark Albright, John Locatelli, Fred Sanders, and the two anonymous reviewers provided insightful comments that enhanced the scope and quality of this manuscript.

REFERENCES

Andersen, P., 1978: On the development and structure of the rolled-up and the bent-back occlusion. *Meteor. Ann.*, 7(4), 79–131.

Anderson, R. K., J. P. Ashman, F. Bittner, G. R. Farr, E. W. Ferguson, V. J. Oliver, and A. H. Smith, 1969: *Application of Meteorological Satellite Data in Analysis and Forecasting.* ESSA Tech. Rep. NESC 51, Washington, D.C. 330 pp.

Arakawa, H., 1952: The characteristic structure of the occluded frontal typhoon in the late fall other than the occlusion of wave-shaped frontal perturbations. *J. Japan Meteor. Soc.*, **30**(7), 211–215.

Atkinson, B. W., and P. A. Smithson, 1974: Meso-scale circulations and rainfall patterns in an occluding depression. *Quart. J. Roy. Meteor. Soc.*, **100**, 3–22.

Bergeron, T., 1928: Uber die dreidimensionale verknupfende Wetteranalyse. *Geophys. Publik.*, **5**, 1–111.

——, 1937: On the physics of fronts. *Bull. Amer. Meteor. Soc.*, **18**, 265–275.

——, 1959: Methods in scientific weather analysis and forecasting: An outline in the history of ideas and hints at a program. *The Atmosphere and Sea in Motion: Scientific Contributions to the Rossby Memorial Volume*, B. Bolin, Ed., Rockefeller Institute Press, 440–474.

Bjerknes, J., 1930: Practical examples of polar-front analysis over the British Isles in 1925–6. *Geophys. Mem.*, **50**, 51 pp.

——, 1935: Investigations of selected European cyclones by means of serial ascents. *Geophys. Publik.*, **11**(4), 1–18.

——, 1951: Extratropical cyclones. *Compendium of Meteorology.* Amer. Meteor. Soc., 577–598.

——, and H. Solberg, 1922: Life cycle of cyclones and the polar front theory of atmospheric circulation. *Geophys. Publik.*, **3**(1), 1–18.

——, and E. Palmén, 1937: Investigations of selected European cyclones by means of serial ascents. *Geophys. Publik.*, **12**, 1–62.

Browning, K. A., and G. A. Monk, 1982: A simple model for the synoptic analysis of cold fronts. *Quart. J. Roy. Meteor. Soc.*, **108**, 435–452.

——, and F. F. Hill, 1985: Mesoscale analysis of a polar trough interacting with a polar front. *Quart. J. Roy. Meteor. Soc.*, **111**, 445–462.

——, M. E. Hardman, T. W. Harrold, and C. W. Pardoe, 1973: The structure of rainbands within a mid-latitude depression. *Quart. J. Roy. Meteor. Soc.*, **99**, 215–231.

Carleton, A. M., 1985: Satellite climatological aspects of the "polar low" and the "instant occlusion." *Tellus*, **37A**, 433–450.

Carr, J. A., 1951: An occluding wave, 7 October 1951. *Mon. Wea. Rev.*, **79**, 200–204.

Donall, E. G., M. A. Shapiro, and P. J. Neiman, 1991: Frontogenesis in a rapidly intensifying extratropical marine cyclone. *First International Symp. on Winter Storms.* New Orleans, Amer. Meteor. Soc., 436 pp.

Douglas, C. K. M., 1929: Some aspects of surfaces of discontinuity. *Quart. J. Roy. Meteor. Soc.*, **55**, 123–151.

Elliott, R. D., 1958: California storm characteristics and weather modification. *J. Meteorol.*, **15**, 486–493.

——, and E. L. Hovind, 1964: On convection bands within Pacific Coast storms and their relation to storm structure. *J. Appl. Meteor.*, **3**, 143–154.

——, and ——, 1965: Heat, water, and vorticity balance in frontal zones. *J. Appl. Meteor.*, **4**, 196–211.

Galloway, J. L., 1958: The three-front model: Its philosophy, nature, construction and use. *Weather*, **13**, 3–10.

——, 1960: The three-front model, the developing depression and the occluding process. *Weather*, **15**, 293–301.

German, K. E., 1959: An investigation of the occlusion process near the earth's surface. M.S. thesis, University of Washington, 47 pp.

Godske, C. L., T. Bergeron, J. Bjerknes, and R. C. Bundgaard, 1957: *Dynamic Meteorology and Weather Forecasting.* American Meteorological Society, 530 pp.

Godson, W. L., 1951: Synoptic properties of frontal surfaces. *Quart. J. Roy. Meteor. Soc.*, **77**, 633–653.

Hertzman, O., and P. V. Hobbs, 1988: The mesoscale and microscale structure and organization of clouds and precipitation in midlatitude cyclones. Part XIV: Three-dimensional airflow and vorticity budget of rainbands in a warm occlusion. *J. Atmos. Sci.*, **45**, 893–914.

Hobbs, P. V., R. A. Houze, Jr., and T. J. Matejka, 1975: The dynamical and microphysical structure of an occluded frontal system and its modification by orography. *J. Atmos. Sci.*, **32**, 1542–1562.

——, J. D. Locatelli, and J. E. Martin, 1990: Cold fronts aloft and the forecasting of precipitation and severe weather east of the Rocky Mountains. *Wea. Forecasting*, **5**, 613–626.

Hoskins, B. J., 1976: Baroclinic waves and frontogenesis Part I: Introduction and Eady waves. *Quart. J. Roy. Meteor. Soc.*, **102**, 103–122.

——, and N. V. West, 1979: Baroclinic waves and frontogenesis Part II: Uniform potential vorticity jet flows—Cold and warm fronts. *J. Atmos. Sci.*, **36**, 1663–1680.

Houze, R. A., Jr., J. D. Locatelli, and P. V. Hobbs, 1976: Dynamics and cloud microphysics of the rainbands in an occluded frontal systems. *J. Atmos. Sci.*, **33**, 1921–1936.

Huschke, R. E., 1959: *Glossary of Meteorology.* Amer. Meteor. Soc., 638 pp.

Jewell, R., 1981: Tor Bergeron's first year in the Bergen School: Towards an historical appreciation. *Contributions to Current Research in Geophysics, Vol. 10. Weather and Weather Maps: A Volume Dedicated to the Memory of Tor Bergeron*, G. H. Lilequist, Ed., Birkhäuser Verlag, 474–490.

Keyser, D., 1986: Atmospheric fronts: An observational perspective. *Mesoscale Meteorology and Forecasting*, P. S. Ray, Ed., Amer. Meteor. Soc., 216–258.

——, and M. A. Shapiro, 1986: A review of the structure and dynamics of upper-level frontal zones. *Mon. Wea. Rev.*, **114**, 452–499.

——, B. D. Schmidt, and D. G. Duffy, 1989: A technique for representing three-dimensional vertical circulations in baroclinic disturbances. *Mon. Wea. Rev.*, **117**, 2463–2494.

Kreitzberg, C. W., 1964: The structure of occlusions as determined from serial ascents and vertically-directed radar. *Rep. AFCRL-64-26*, Air Force Cambridge Research Laboratory, Bedford, MA, 121 pp.

——, 1968: The mesoscale wind field in an occlusion. *J. Appl. Meteor.*, **7**, 53–67.

——, and H. A. Brown, 1970: Mesoscale weather systems within an occlusion. *J. Appl. Meteor.*, **9**, 419–432.

Kuo, Y.-H., and R. J. Reed, 1988: Numerical simulation of an explosively deepening cyclone in the Eastern Pacific. *Mon. Wea. Rev.*, **116**, 2081–2105.

——, M. A. Shapiro, and E. G. Donall, 1991: The interaction between baroclinic and diabatic processes in a numerical simulation of a rapidly intensifying extratropical marine cyclone. *Mon. Wea. Rev.*, **119**, 368–384.

——, R. J. Reed, and S. Low-Nam, 1992: Thermal structure and airflow in a model simulation of an occluded marine cyclone. *Mon. Wea. Rev.*, **120**, 2280–2297.

Kurz, M., 1988: Development of cloud distribution and relative motions during the mature and occlusion stage of a typical cyclone development. *Palmén Memorial Symposium on Extratropical Cyclones: Reprints.* Amer. Meteor. Soc., 201–204.

Locatelli, J. D., P. V. Hobbs, and J. A. Werth, 1982: Mesoscale structures of vortices in polar air streams. *Mon. Wea. Rev.*, **110**, 1417–1433.

——, J. M. Sienkiewicz, and P. V. Hobbs, 1989: The organization and structure of clouds and precipitation on the mid-Atlantic coast of the United States. I: Synoptic evolution of a frontal system from the Rockies to the Atlantic Coast. *J. Atmos. Sci.*, **46**, 1337–1348.

Lynott, R. E., and O. P. Cramer, 1966: Detailed analysis of the 1962 Columbus Day windstorm in Oregon and Washington. *Mon. Wea. Rev.*, **94**, 105–117.

Mass, C. F., and D. M. Schultz, 1993: The structure and evolution of a simulated midlatitude cyclone over land. *Mon. Wea. Rev.*, **121**, 889–917.

Matejka, T. J., 1980: Mesoscale organization of cloud processes in extratropical cyclones. Ph.D. thesis, University of Washington, 86–97.

Matkovski, B. M., and N. P. Shakina, 1982: Mesoscale structure of an occlusion over the central European USSR from data of special measurements. *Meteorologiya I Gidrologiya*, **1**, 24–33.

McClain, E. P., and E. F. Danielsen, 1955: Zonal distribution of baroclinity for three Pacific storms. *J. Meteorol.*, **12**, 314–323.

McGinnigle, J. B., M. V. Young, and M. J. Bader, 1988: The development of instant occlusions in the North Atlantic. *Meteor. Mag.*, **117**, 325–341.

Miller, J. E., 1948: On the concept of frontogenesis. *J. Meteor.*, **5**, 169–171.

Monk, G., 1987: Satellite picture of an instant occlusion. *Weather*, **42**, 14–16.

Mudrick, S. E., 1974: A numerical study of frontogenesis. *J. Atmos. Sci.*, **31**, 869–892.

Nakamura, N., 1989: Dynamics of baroclinic instability in rapid cyclogenesis. Ph.D. thesis, Princeton University, 110 pp.

Palmén, E., 1951: The aerology of extratropical disturbances. *Compendium of Meteorology.* Amer. Meteor. Soc., 599–620.

Penner, C. M., 1955: A three-front model for synoptic analyses. *Quart. J. Roy. Meteor. Soc.*, **81**, 89–91.

Petterssen, S., 1940: *Weather Analysis and Forecasting.* McGraw-Hill, 503 pp.

——, 1956: *Weather Analysis and Forecasting. Vol. 1: Motions and Motion Systems*, 2nd Ed., McGraw-Hill, 428 pp.

Pike, W. S., 1991: An alternative frontal analysis for the storm of 3 February 1990. *Weather*, **46**, 150–151.

Polavarapu, S. M., and W. R. Peltier, 1990: The structure and evolution of synoptic-scale cyclones: Life cycle simulations with a cloud-scale model. *J. Atmos. Sci.*, **47**, 2645–2672.

Postma, K. R., 1948: The formation and the development of occluding cyclones: A study of surface-weather maps. Ph.D. thesis, Utrecht, 57 pp.

Ragette, G., 1984: Analysis of a frontal system over central Europe. *Beitr. Phys. Atmosph.*, **57**, 447–462.

Reed, R. J., 1979: Cyclogenesis in polar air streams. *Mon. Wea. Rev.*, **107**, 38–52.

Saarikivi, P., and T. Puhakka, 1990: The structure and evolution of a wintertime occluded front. *Tellus*, **42A**, 122–139.

Saucier, W. J., 1955: *Principles of Meteorological Analysis.* University of Chicago Press, 438 pp.

Schär, C. J., 1989: Dynamische aspekte der aussertropischen zyklogenese, theorie und numerische simulation im limit der bal-

ancierten strömungssysteme. Dissertation Nr. 8845 der Eidgenossischen Technischen Hochschule, Zurich, 241 pp.

Schultz, D. M., 1990: The structure and evolution of an occluding midlatitude cyclone as diagnosed with a mesoscale numerical model. M.S. thesis, Department of Atmospheric Sciences, University of Washington, 316 pp.

Seaman, N. L., 1987: Program TRAJEC: Documentation and users guide. PSU-NWPLIB-0010-87, 95 pp.

Shapiro, M. A., and D. Keyser, 1990: Fronts, jet streams and the tropopause. *Extratropical Cyclones: The Erik Palmén Memorial Volume.* C. W. Newton and E. O. Holopainen, Eds., Amer. Meteor. Soc., 167–191.

Smith, R. K., and M. J. Reeder, 1988: On the movement and low-level structure of cold fronts. *Mon. Wea. Rev.*, **116,** 1927–1944.

Takayabu, I., 1986: Roles of the horizontal advection on the formation of surface fronts and on the occlusion of a cyclone developing in the baroclinic westerly jet. *J. Meteor. Soc. Japan,* **64**(3), 329–345.

Wallace, J. M., and P. V. Hobbs, 1977: *Atmospheric Science: An Introductory Survey.* Academic Press, 467 pp.

Wang, P-Y., and P. V. Hobbs, 1983: The mesoscale and microscale structure and organization of clouds and precipitation in midlatitude cyclones. X: Wavelike rainbands in an occlusion. *J. Atmos. Sci.*, **40,** 1950–1964.

Wexler, H., 1935: Analysis of a warm-front-type occlusion. *Mon. Wea. Rev.*, **63,** 213–221.

Whitaker, J. S., L. W. Uccellini, and K. F. Brill, 1988: A model-based diagnostic study of the rapid development phase of the President's Day cyclone. *Mon. Wea. Rev.*, **116,** 2337–2365.

Zwatz-Meise, V., and G. Hailzl, 1983: A cloud formation process contradictory to the classical occlusion development investigated with satellite images and model output parameters. *Arch. Met. Geoph. Biocl., Ser. A,* **32,** 119–127.

APPENDIX

Survey of Occluded Front Studies

Study	Environment	Observed structures	Temperature structure favors
Bjerknes (1935)	M	WT	WT
Wexler (1935)	C	WT	CT
Bjerknes and Palmén (1937)	M	WT	WT
Carr (1951)	C	X	CT
Palmén (1951)	C	X	X
McClain and Danielsen (1955)	M	WT	CT
Elliott (1958)	M	CT[a,b]	X
German (1959)	C	X	CT
Kreitzberg (1964)	M	4WT	X
Elliott and Hovind (1964, 1965)	M	WT[b]	X
Lynott and Cramer (1966)	M	WT	WT
Kreitzberg (1968)	C	WT	X
Kreitzberg and Brown (1970)	C	WT	X
Atkinson and Smithson (1974)	M	WT	X
Hobbs et al. (1975)	M	CT[b]	CT
Houze et al. (1976)	M	2WT	WT?
Andersen (1978)	M	WT	WT
Matejka (1980)	M	CT[c]	CT
Matkovski and Shakina (1982)	C	WT	WT
Wang and Hobbs (1983)	M	WT	CT?
Ragette (1984)	C	WT	X
Hertzman and Hobbs (1988)	M	WT	CT?
Kuo and Reed (1988)	M		CT
Kurz (1988)	C	WT	CT
Saarikivi and Puhakka (1990)	M		WT
Shapiro and Keyser (1990)	M		4WT
Mass and Schultz (1992)	C	WT	CT

[a] Only a schematic based on observed storm structures.

[b] No elevated warm front.

[c] May be reanalyzed as a warm-type occlusion.

C—continental cyclone; M—marine cyclone; WT—warm-type occlusion; CT—cold-type occlusion; ?—considerable uncertainty; X—unable to determine.